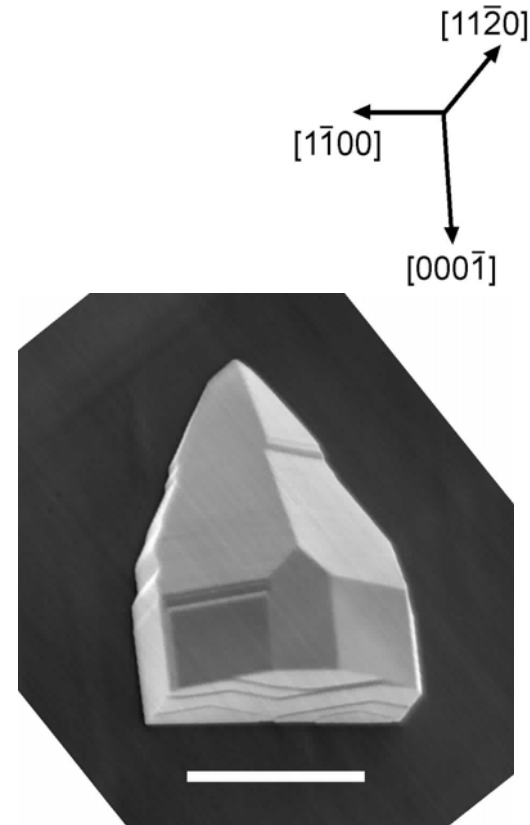


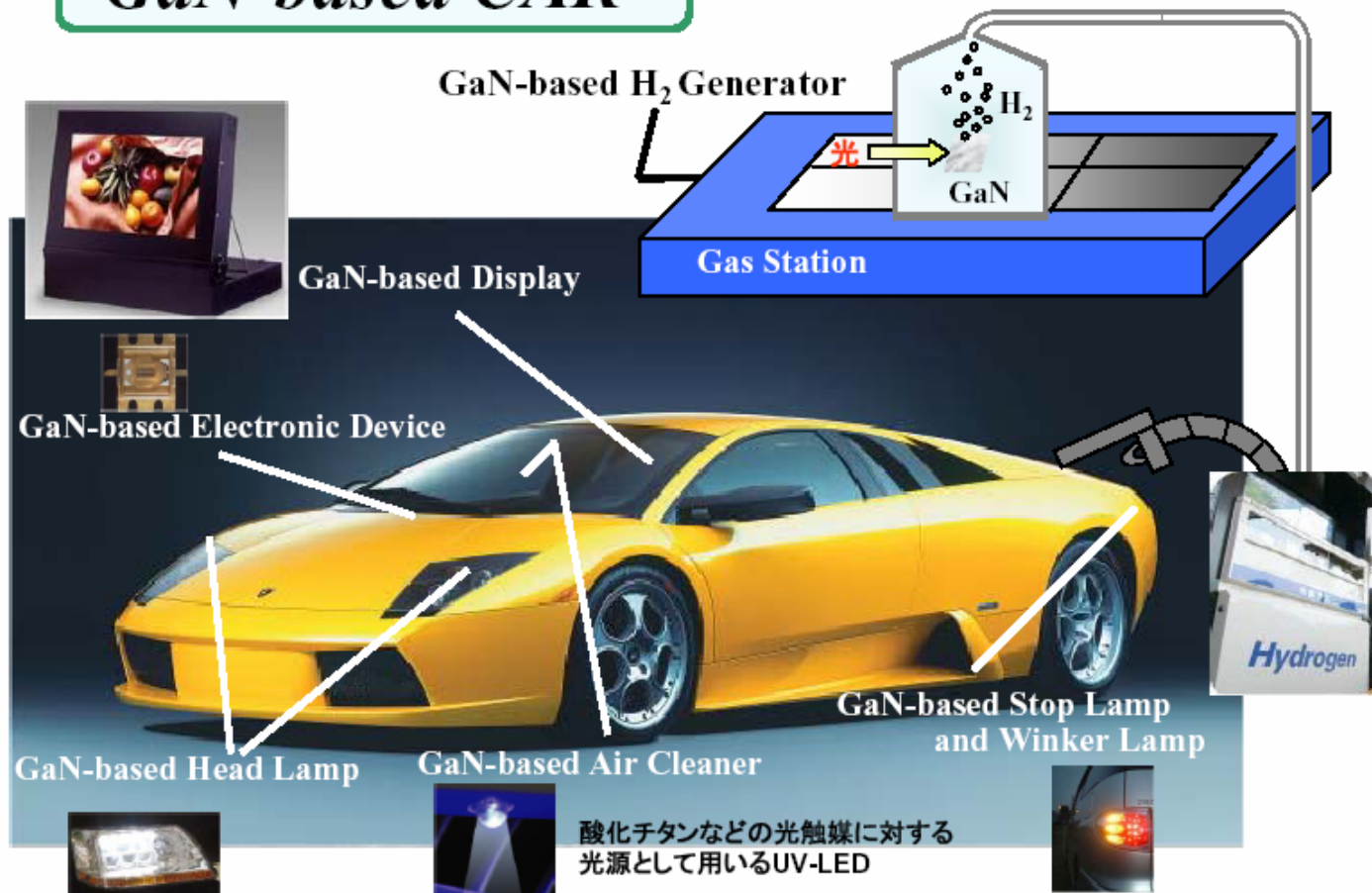
# *New Faces of GaN: Growth, Doping and Devices*

**James S. Speck**  
Materials Department  
University of California  
Santa Barbara, CA

LEO of a-GaN from circular opening



# GaN-based CAR



# Personnel

## MOCVD

Mike Craven (now Lumileds)  
Arpan Chakraborty (now Cree)

Bilge Imer

John Kaeding - poster

KC Kim - poster

Don Lee

Matt Schmidt

## HVPE

Troy Baker - poster

Asako Hirai - poster

Ben Haskell

## MBE

Mel McLaurin - poster

Siddharth Rajan

ManHoi Wong

## TEM

Feng Wu

Yuan Wu

## Staff

Paul Fini

Stacia Keller

## Faculty

Steve DenBaars

Umesh Mishra

Shuji Nakamura

Jim Speck

## Key Collaborators

S.F. Chichibu (Tsukuba)

H. Grahn (PDI)

M. Wraback (ARL)

## \$\$\$

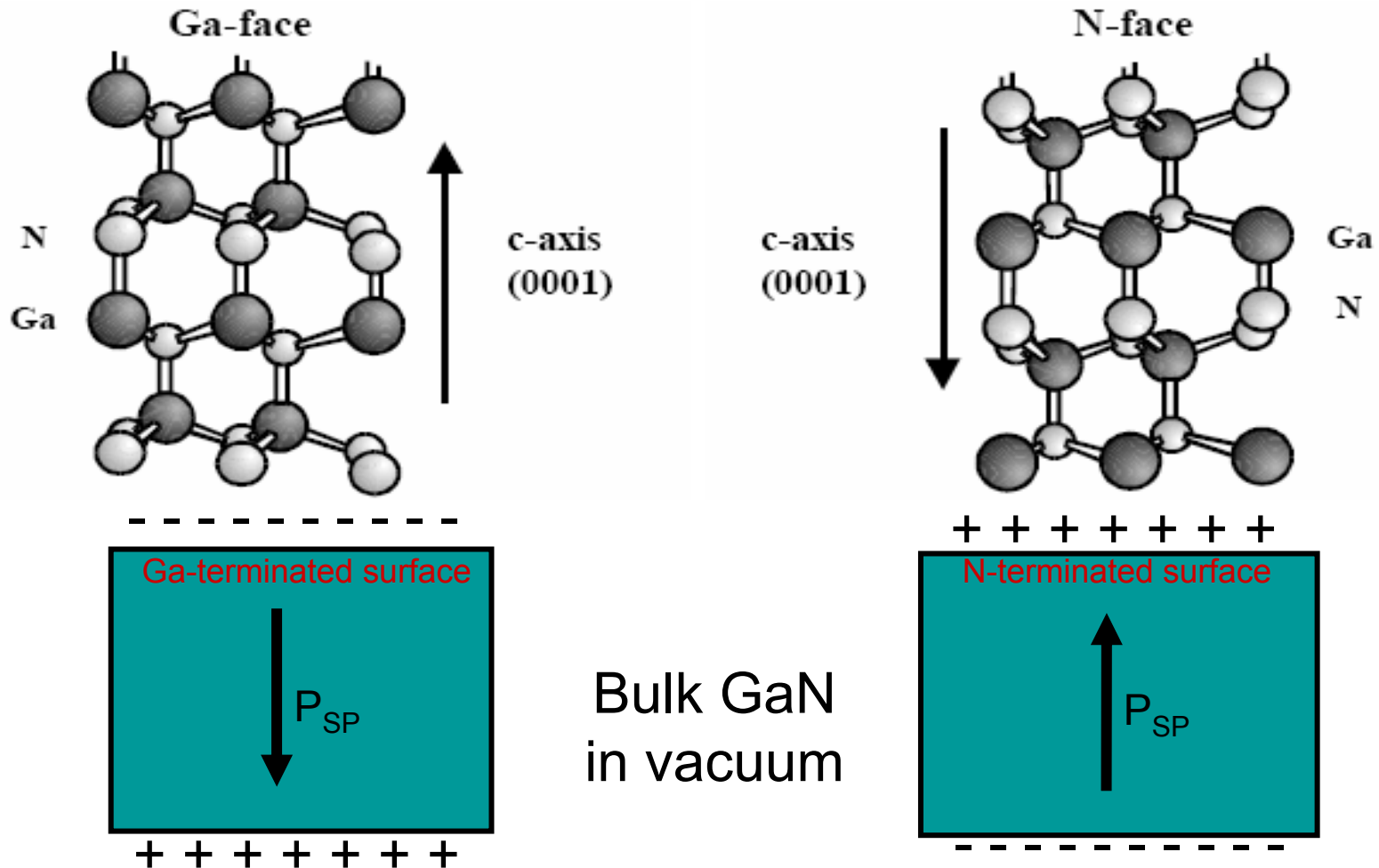
JST – ERATO

UCSB SSLDC

AFOSR

ONR

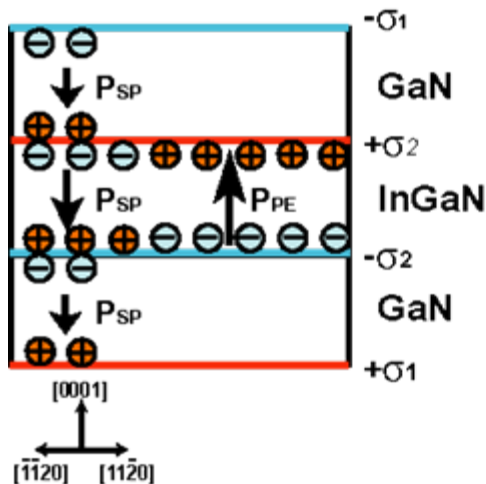
# Wurtzite Nitrides Crystal Symmetry



Reversed direction of polarization

# Motivation – Polarization Effects

on C Plane (Ga Face)



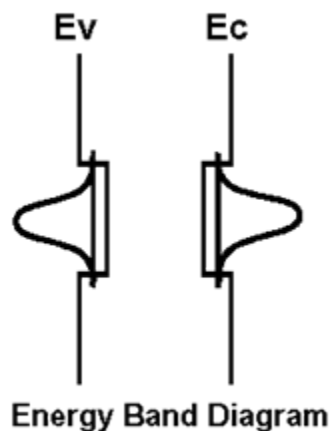
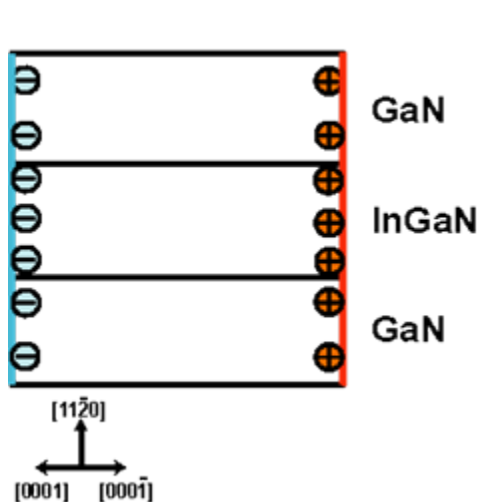
Spontaneous and piezoelectric polarization cause:

1. band bending
2. charge separation in QW



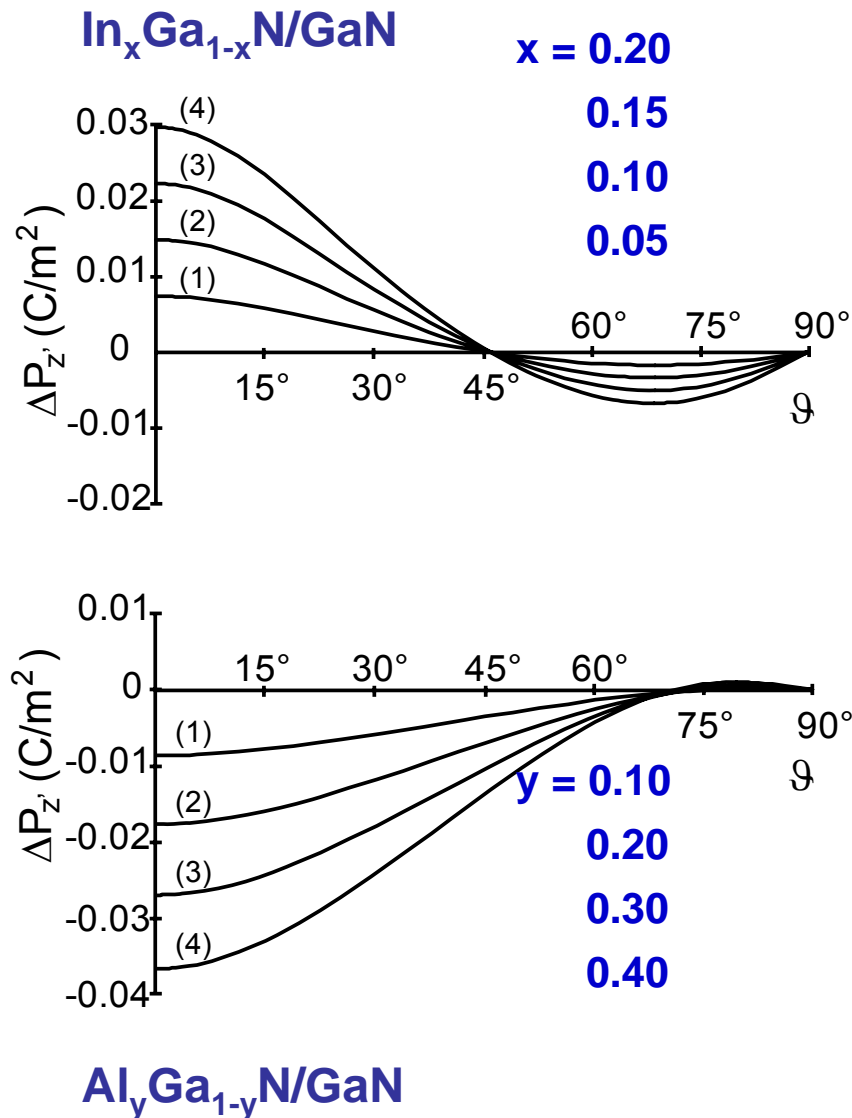
- Emission red shift
- Low recombination efficiency
- High threshold current

on A Plane



**Growth on non-polar, semi-polar GaN will solve these problems**

# Total Polarization Discontinuity



**Calculated total polarization change**

In<sub>x</sub>Ga<sub>1-x</sub>N coherently strained to GaN

Al<sub>y</sub>Ga<sub>1-y</sub>N coherently strained to GaN

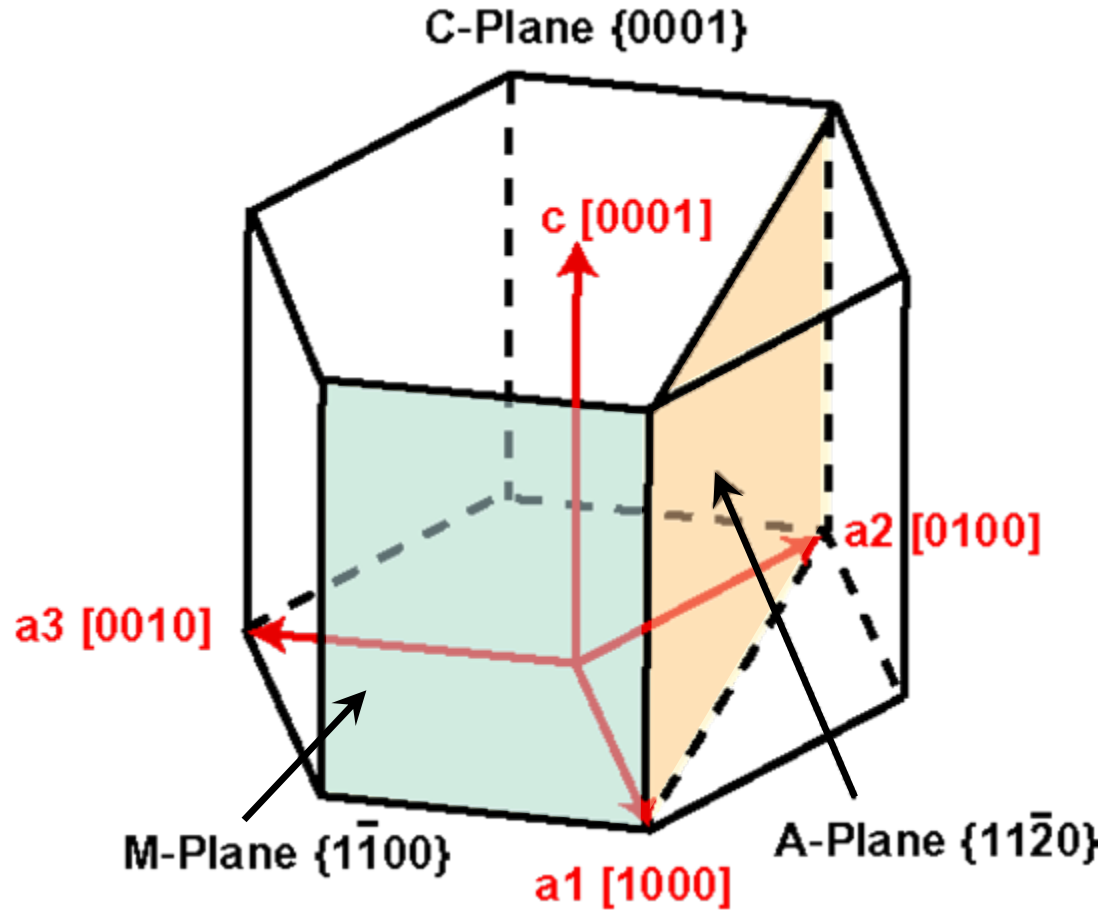
**Polarization discontinuity**

Spontaneous

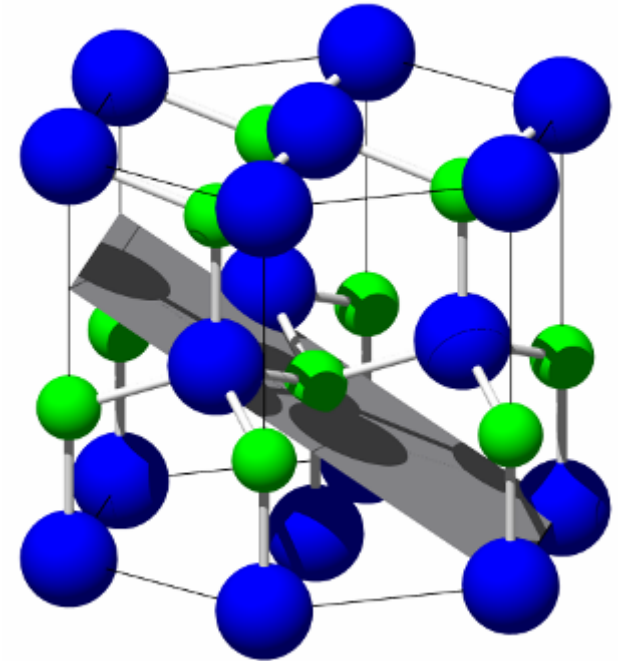
Piezoelectric

# GaN Crystal Structure

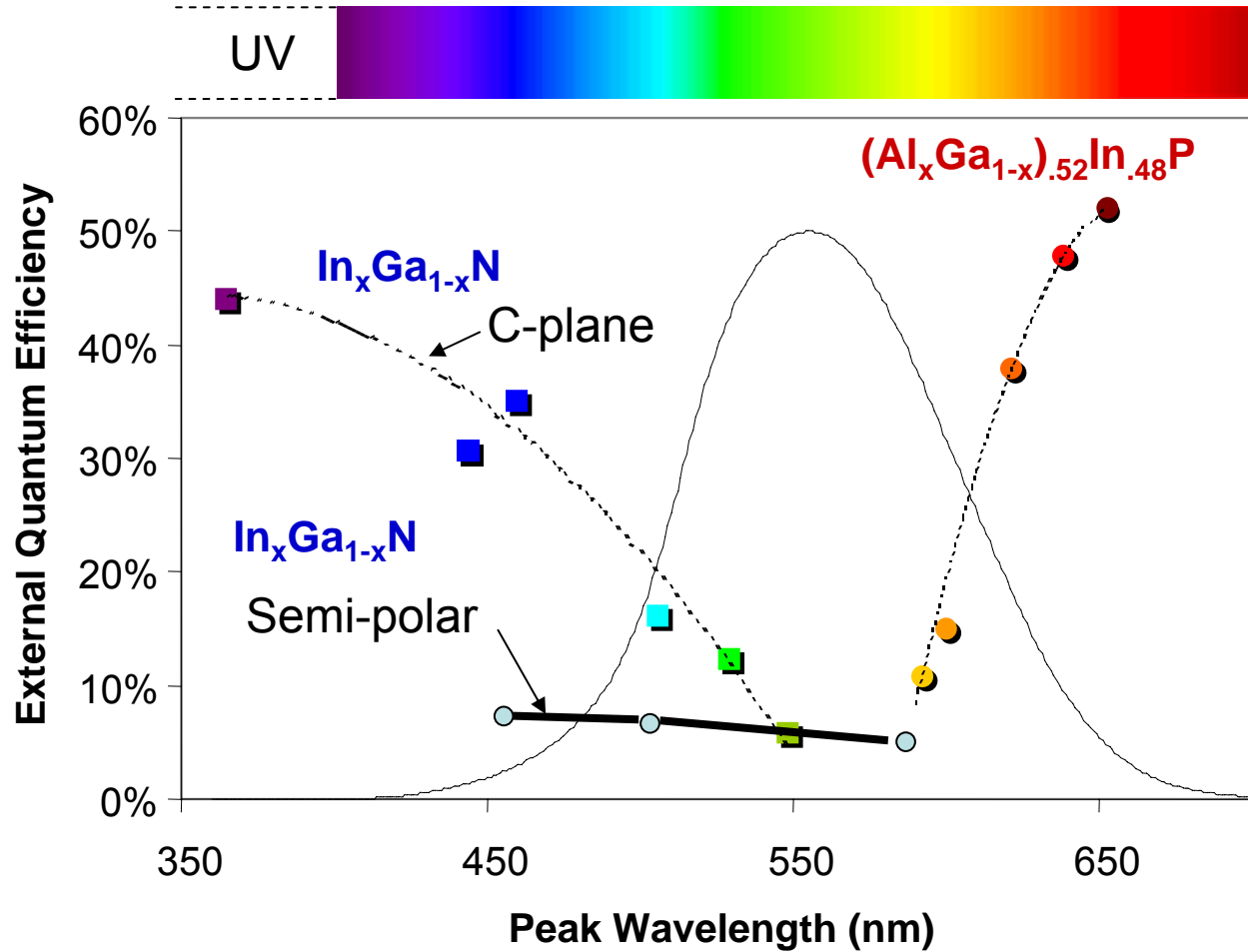
## Non-Polar Planes



## Semi-Polar Planes



# LED Efficiency



# Non-Polar Growth - Summary

## Systems

- $a$ -GaN /  $r$ -Al<sub>2</sub>O<sub>3</sub> (MOCVD, HVPE and MBE)
- $a$ -GaN /  $a$ -SiC (MOCVD, MBE, MBE → HVPE)
- $m$ -GaN /  $m$ -SiC (MOCVD and MBE, MBE → HVPE)
- $m$ -GaN / (001) LiAlO<sub>2</sub> (HVPE, MBE → HVPE)

Exchange of MBE, MOCVD and HVPE material

*'Mix and match'*

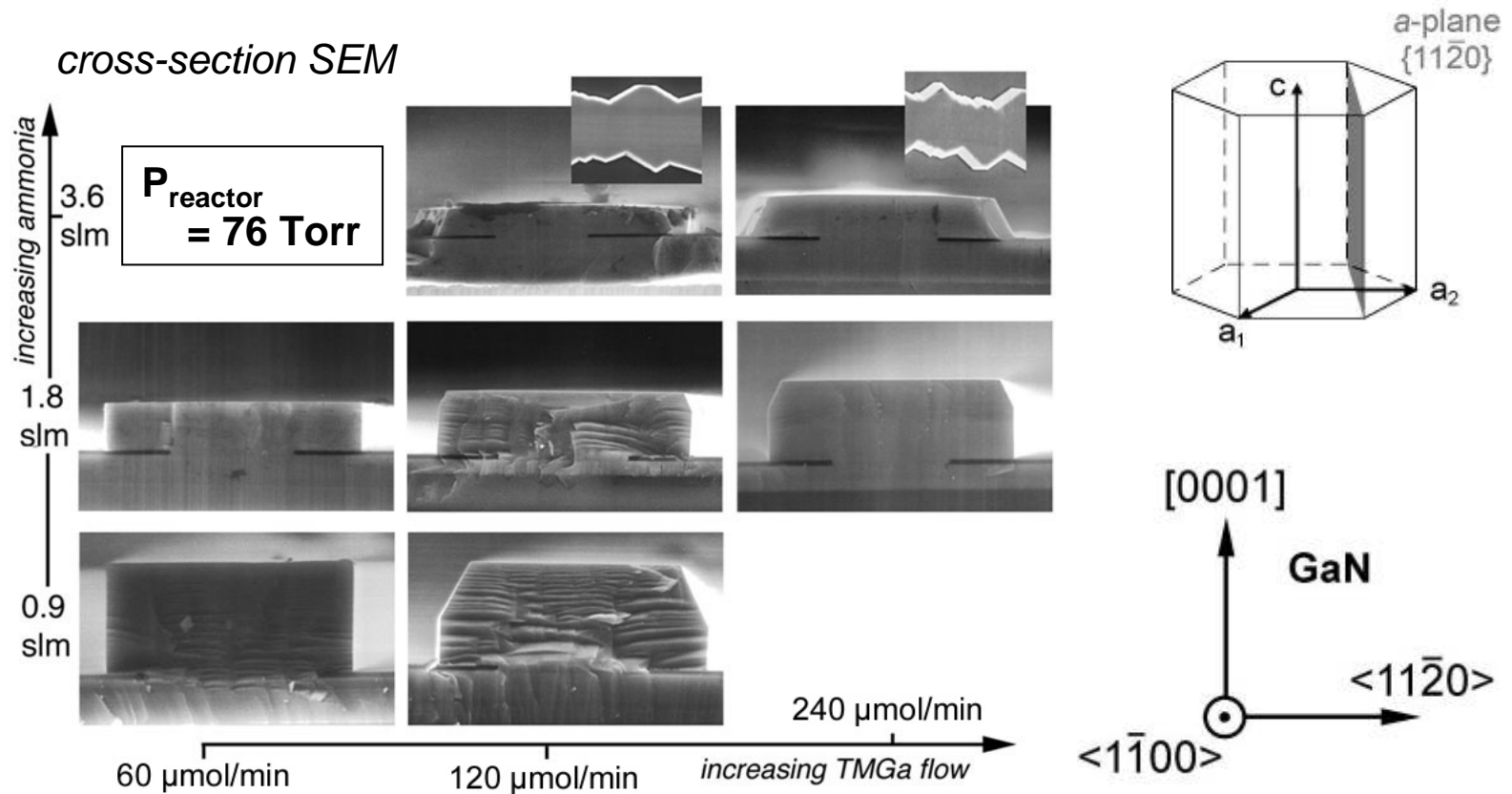
(e.g., MBE  $m$ -GaN/LiAlO<sub>2</sub> templates for HVPE → MOCVD)

## Research Topics

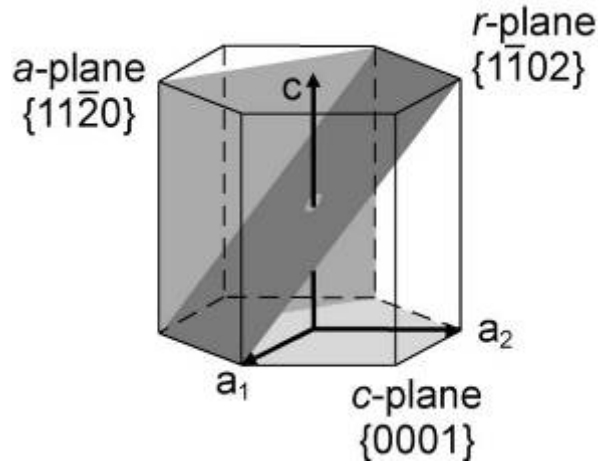
- Growth mode and growth mechanisms
- Morphology
- Defect generation and structure
- Optical properties
- Doping
- Heterostructures
- Devices

# a-GaN Growth: ... the idea ...

- a-plane surfaces encountered in the lateral overgrowth of c-plane GaN

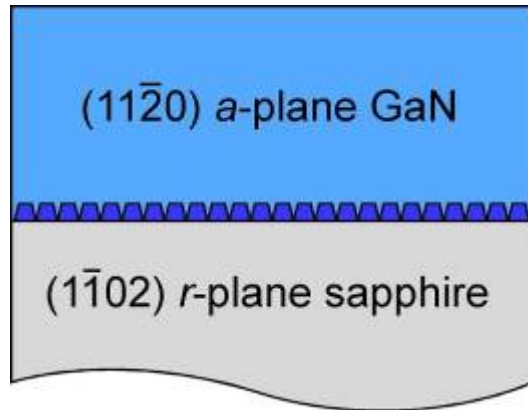


# Nonpolar *a*-GaN on *r*-plane Sapphire



## *a*-GaN grown on *r*-sapphire via MOCVD

- Previous efforts produced faceted films
- Planar films attained using two-step growth



### *GaN Epitaxial Film*

V/III: 300 – 1300

$T_g$ : ~1120°C

g.r.: 2 – 9 Å/s

P: ≤ 100 Torr

### *GaN Nucleation Layer*

V/III: 2500

$T_g$ : ~600°C

t: ~20 nm

### *...compare to c-GaN Epitaxy...*

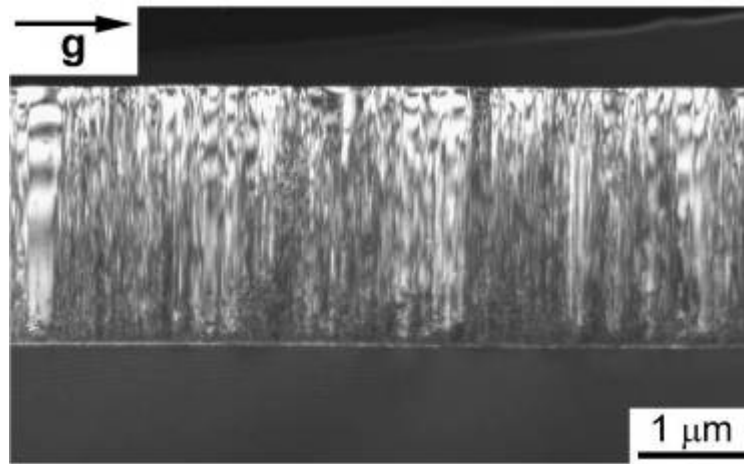
V/III: 2000 – 3500

$T_g$ : ~1090°C

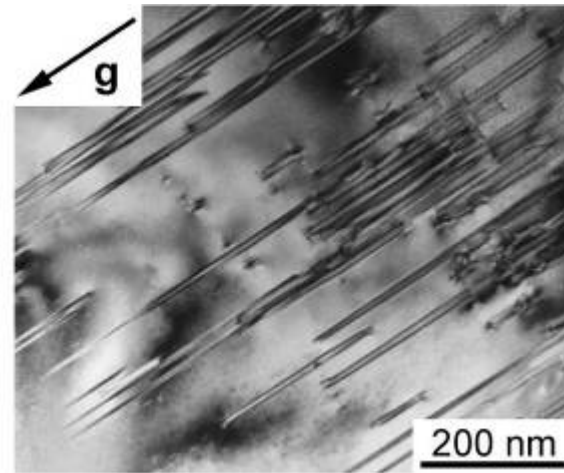
P: 76-760 Torr

# a-GaN Microstructure

*x-section  
TEM*



*plan-view  
TEM*



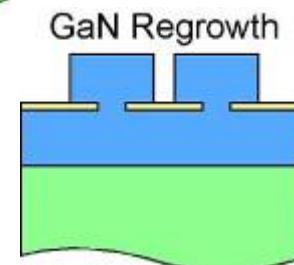
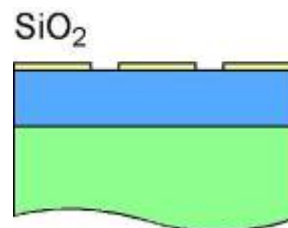
- $2.6 \times 10^{10} \text{ cm}^{-2}$  threading dislocation (TD) density
  - Common  $[11\bar{2}0]$  TD line direction
- $3.8 \times 10^5 \text{ cm}^{-1}$  basal plane stacking fault density
  - Faults aligned perpendicular to the  $c$ -axis  $[0001]$

# Lateral Epitaxial Overgrowth

- Lateral overgrowth techniques effectively reduce threading dislocation densities in *c*-plane GaN

- **The LEO Process...**

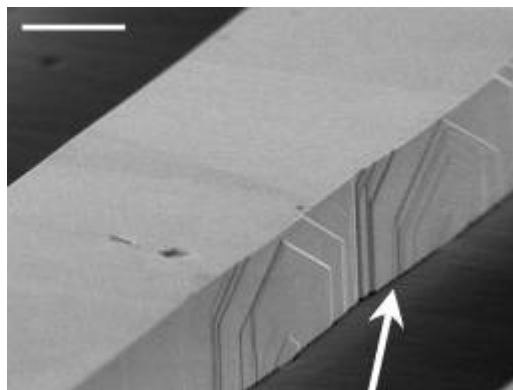
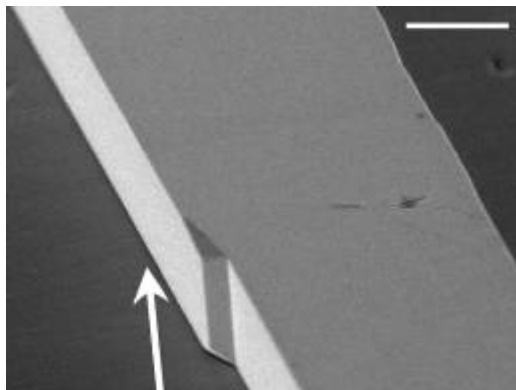
- Initial MOCVD Growth
  - GaN template layer
- Dielectric Mask Pattern
  - 200 nm PECVD SiO<sub>2</sub>
- MOCVD LEO Regrowth
  - Same conditions as planar *a*-GaN growth



# Polarity Effects

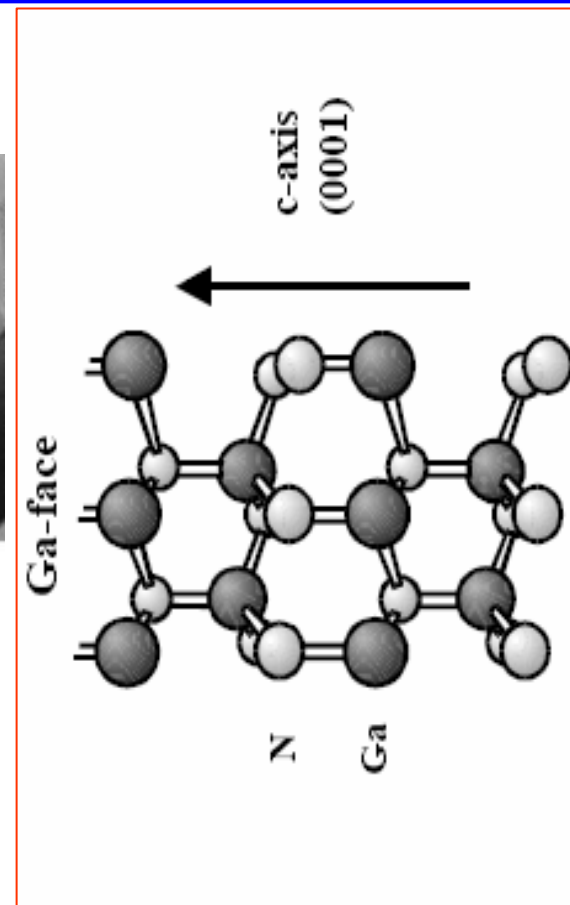
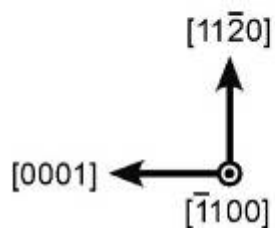
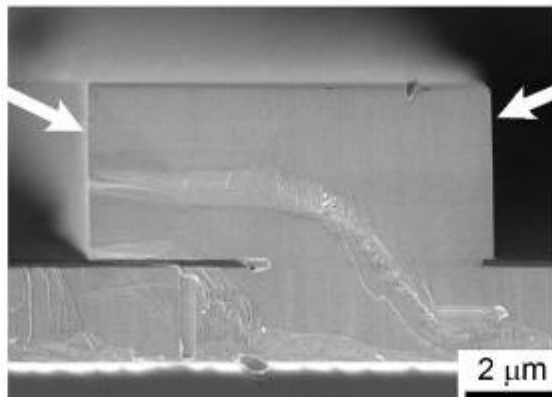
SEM

Scale bar = 3  $\mu\text{m}$



+c-plane  
(0001)  
Ga-face

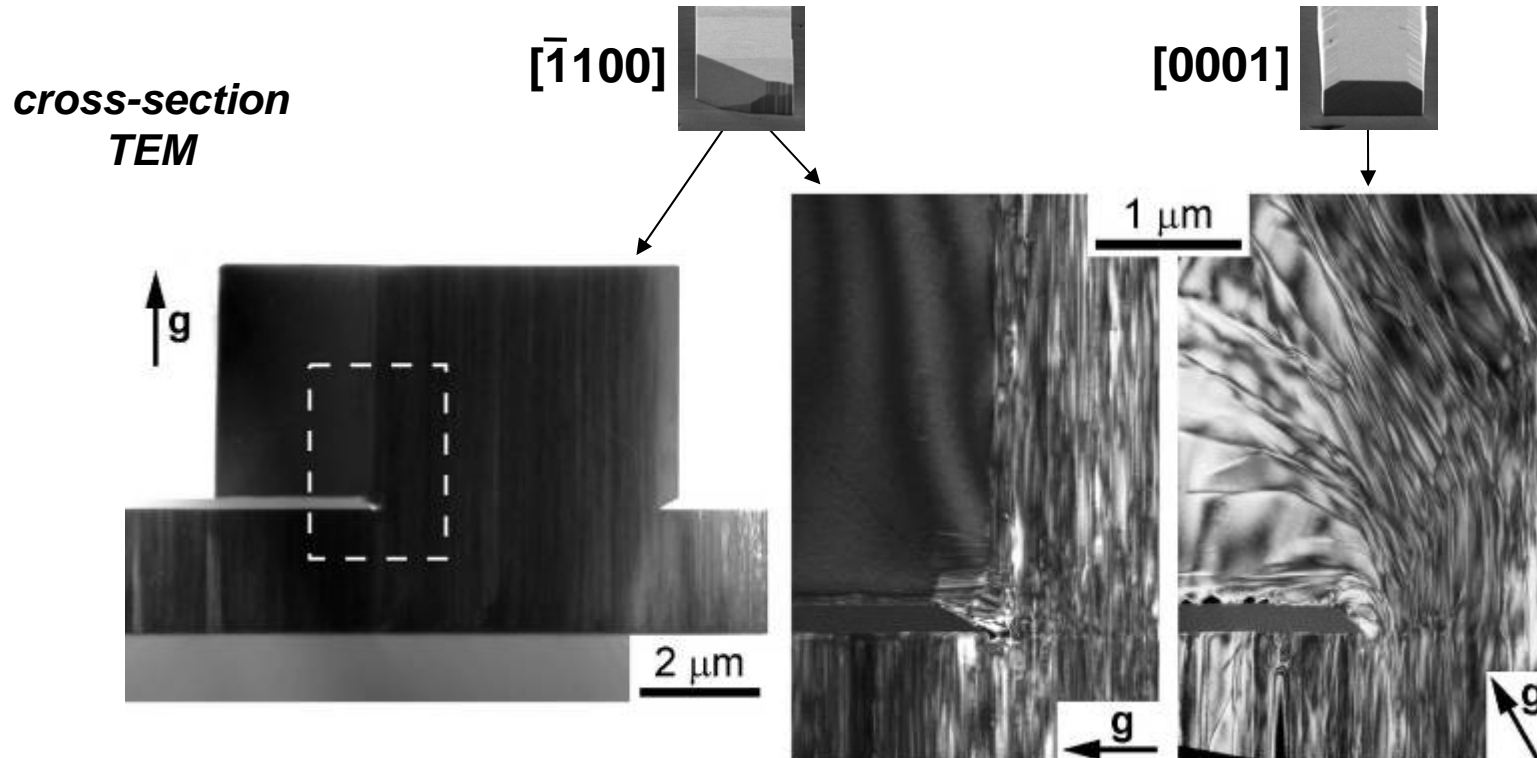
-c-plane  
(000 $\bar{1}$ )  
N-face



**GaN polarity strongly affects lateral growth rate**

- Ga-face sidewall grows  $\sim 10\text{x}$  faster than N-face sidewall

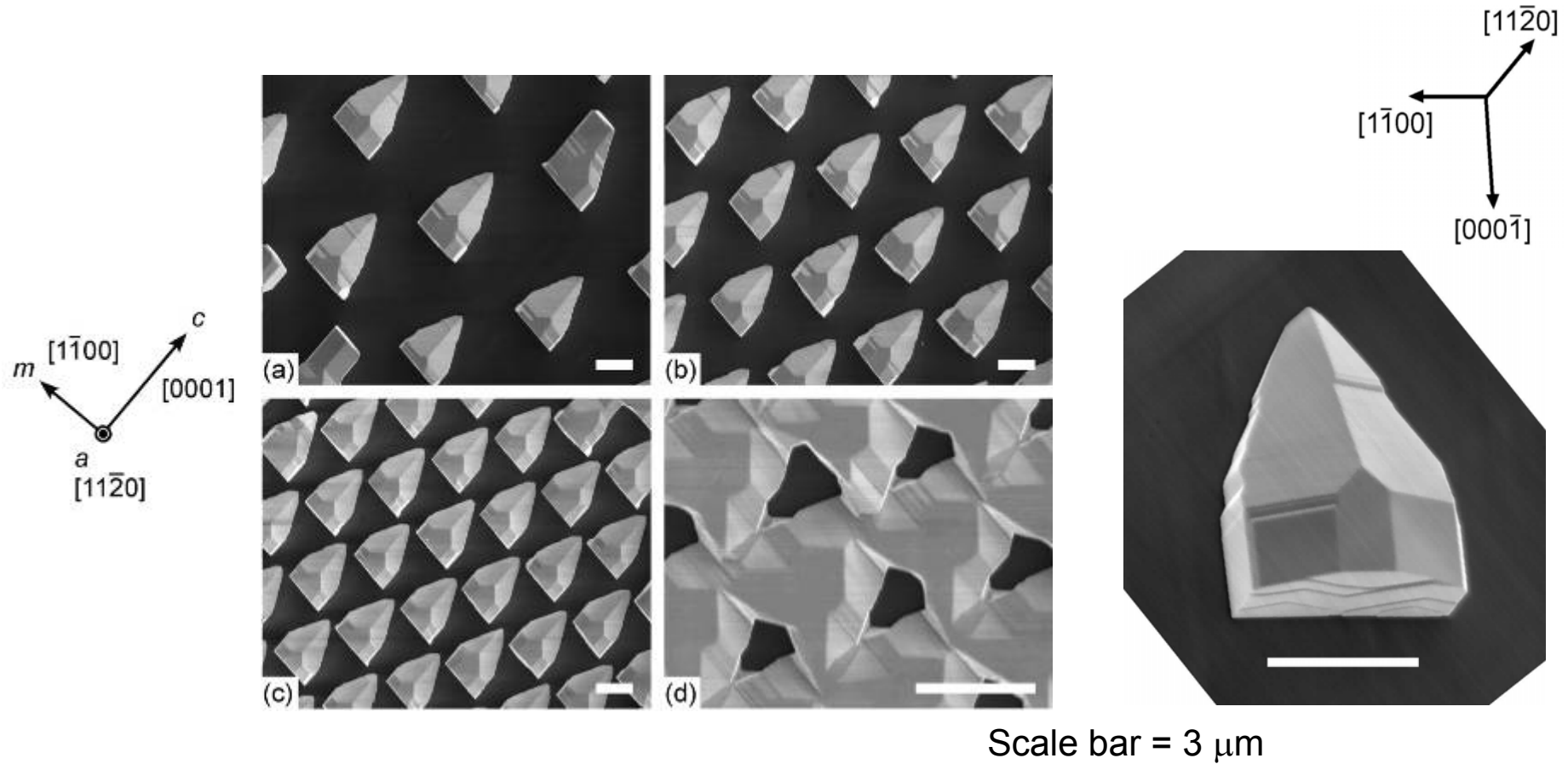
# Dislocation Reduction



- overgrown regions of  $[1\bar{1}00]$  stripes relatively TD free
- dislocations bend into overgrowth from  $[0001]$  stripes

# LEO: Circular Mask Openings

- Stable GaN facets under 'a-plane' MOCVD growth conditions



# LEDs on Planar m-GaN Substrates

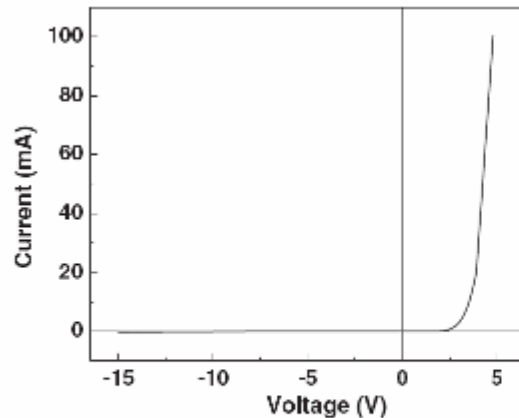


Fig. 1.  $I$ - $V$  characteristic of nonpolar  $m$ -plane LED lamp.

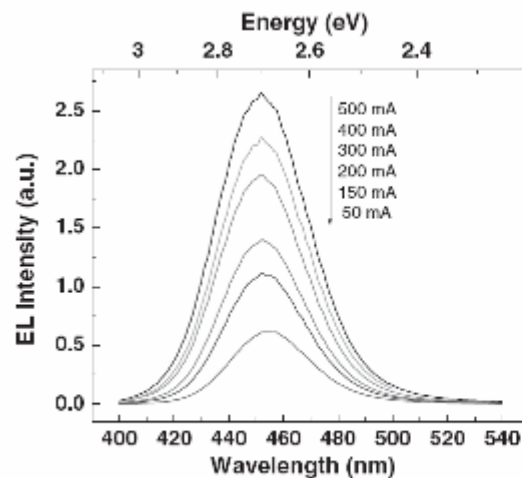


Fig. 2. Emission spectra of LED lamp under pulsed operation.

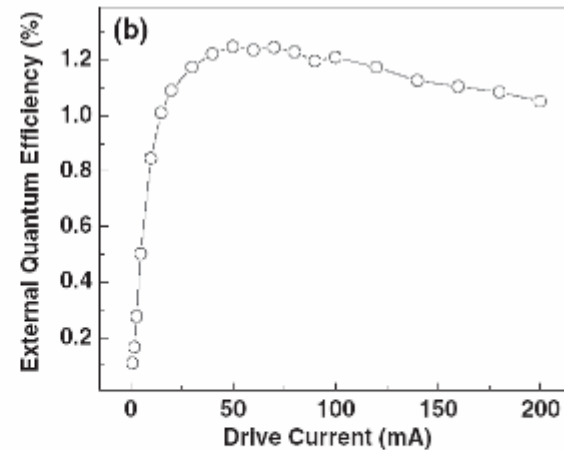
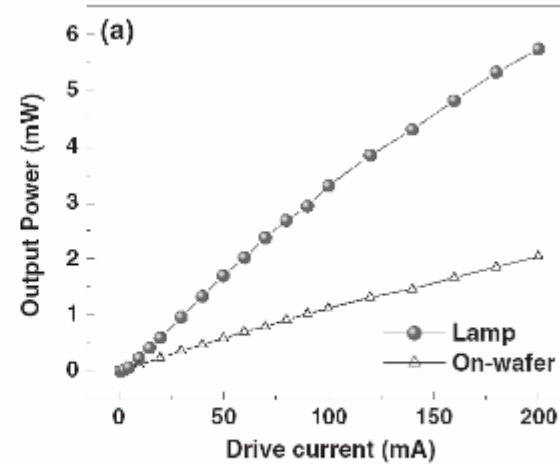
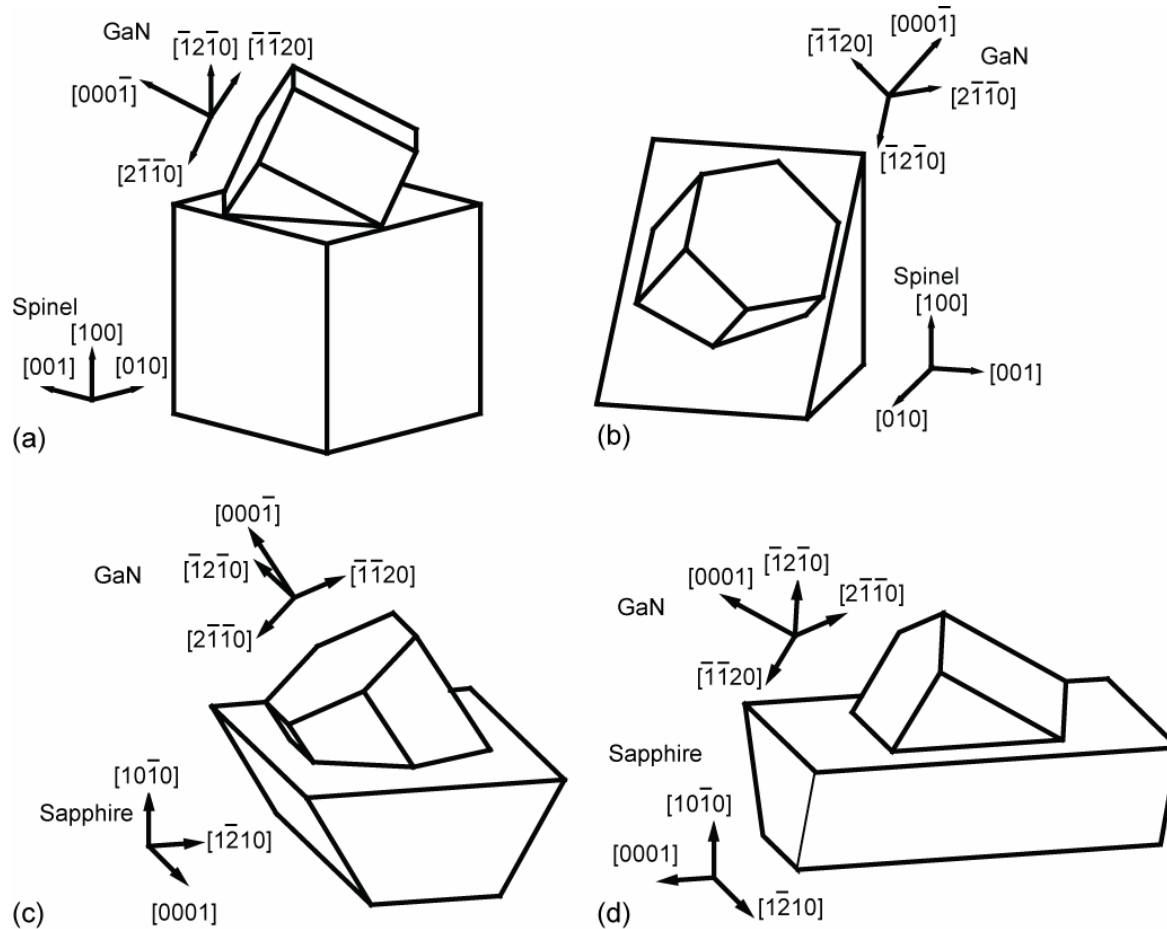


Fig. 3. (a) DC output power versus drive current before and after packaging. (b) Variation in external quantum efficiency with drive current for LED lamp.

# Semi-Polar Orientations



(a)  $(10\bar{1}\bar{1})$ , (b) and (c)  $(10\bar{1}\bar{3})$ , (d)  $(1\bar{1}\bar{2}\bar{2})$  templates

[T.J. Baker *et al.*, Jap. J. Appl. Phys. **44**, L920 (2005)]

# Summary and Prospects

- Routes to non-polar and semi-polar GaN – well demonstrated  
Major challenge: high TD density and SF density
- Defect reduction via LEO, 2S-LEO, SLEO, in situ SiN<sub>x</sub>
- Record p-type doping in MBE GaN on m-plane SiC
- ~1 mW, unoptimized, LEDs on m-plane GaN; semi-polar GaN
- Demonstration of polarized light emission in EL from
  - m-plane LEDs
  - Semi-polar LEDs
- N-face GaN
  - New promise for advanced electronic devices

# MOCVD *a*-Ga<sub>N</sub> LEO: Evidence for *m*-Facet Stability

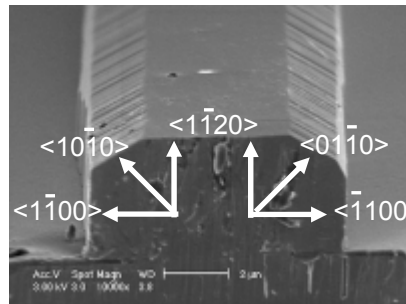
## *a*-Ga<sub>N</sub> LEO with $\langle 0001 \rangle$ stripes

*a* and *m*-facets

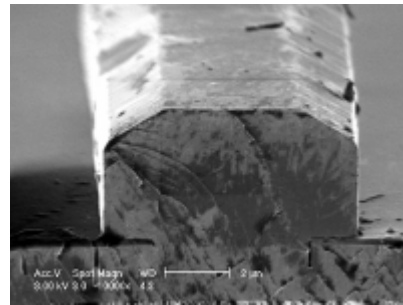
Increasing reactor pressure: loss of *a*-facets, only *m*-facets

Stripe  
orientation

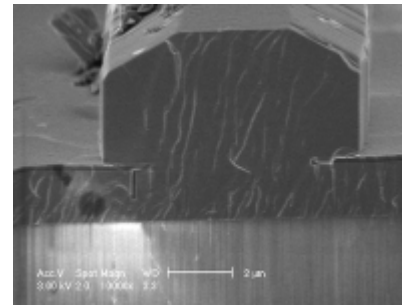
$\langle 0001 \rangle$



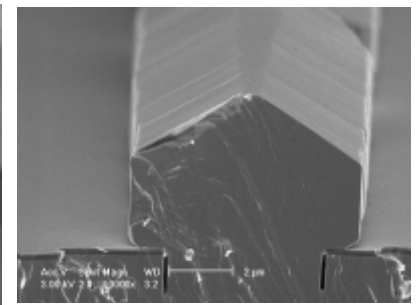
45 Torr



60 Torr

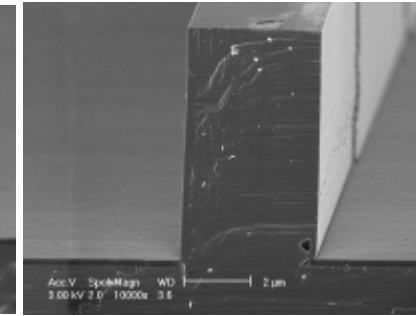
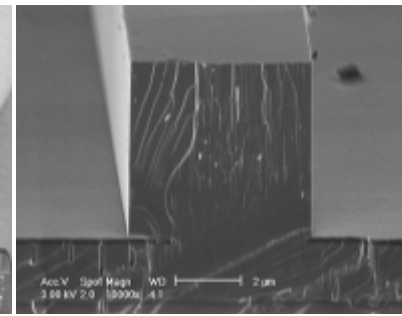
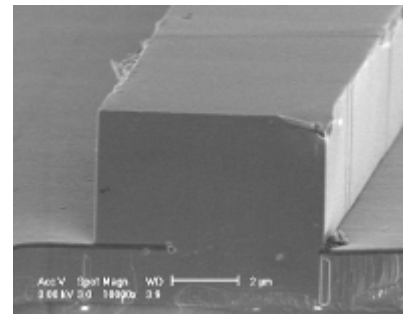
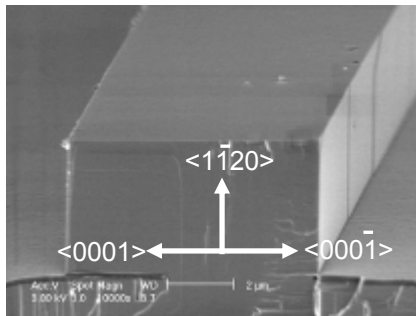


100 Torr



150 Torr

$\langle 1\bar{1}00 \rangle$



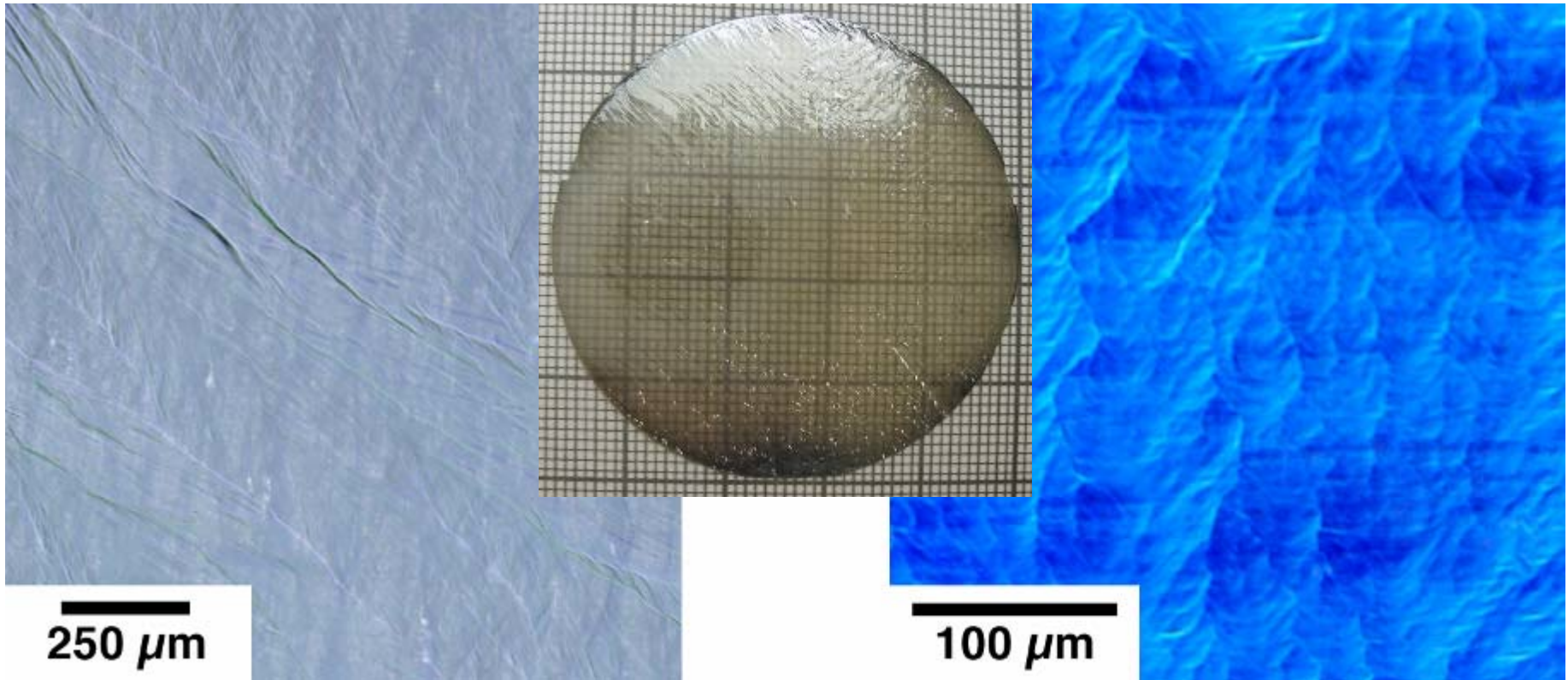
## *a*-Ga<sub>N</sub> LEO with $\langle 1\bar{1}00 \rangle$ stripes

Vertical Ga-face and N-face facets

Increasing reactor pressure: favors vertical growth

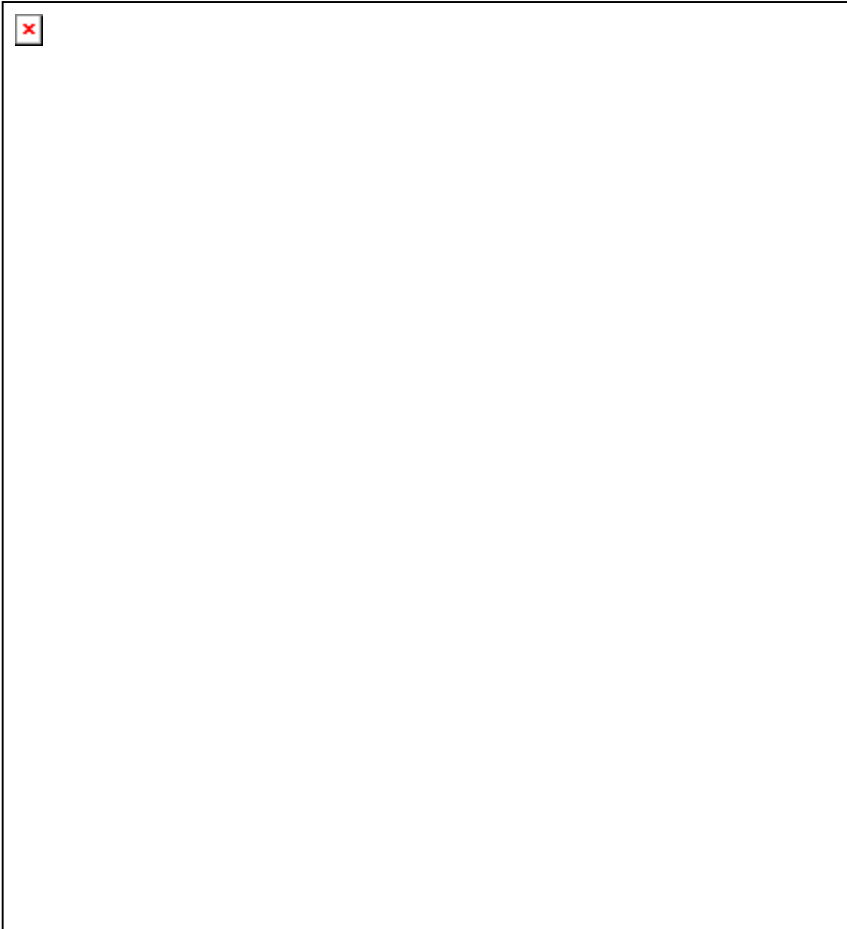
# Planar HVPE m-GaN on LiAlO<sub>2</sub>

Free-standing m-GaN:



- Surfaces characterized by long-range textures, peak to valley < 200 nm.
- Near complete elimination of bulk, crystallographic defects.

# LED on planar *m*-GaN



LED structure grown by MOCVD on ~250  $\mu\text{m}$  thick HVPE **free-standing** *m*-GaN

**MQW parameters:**  
4 nm InGaN well, 16 nm GaN:Si barrier

*n*-GaN: 2.2  $\mu\text{m}$  ( $3 \times 10^{18} \text{ cm}^{-3}$ )

*p*-GaN: 0.3  $\mu\text{m}$  ( $6 \times 10^{17} \text{ cm}^{-3}$ )

*n*-contact: Al/Au (30/200 nm)

*p*-contact: Pd/Au (20/200 nm)

# Polarized Light Emission – EL – *m*-plane GaN LEDs

APPLIED PHYSICS LETTERS 86, 111101 (2005)

## Polarization anisotropy in the electroluminescence of *m*-plane InGaN–GaN multiple-quantum-well light-emitting diodes

N. F. Gardner,<sup>a)</sup> J. C. Kim, J. J. Wierer, Y. C. Shen, and M. R. Krames  
*Advanced Laboratories, Lumileds Lighting, 370 West Trimble Road, San Jose, California 95131*

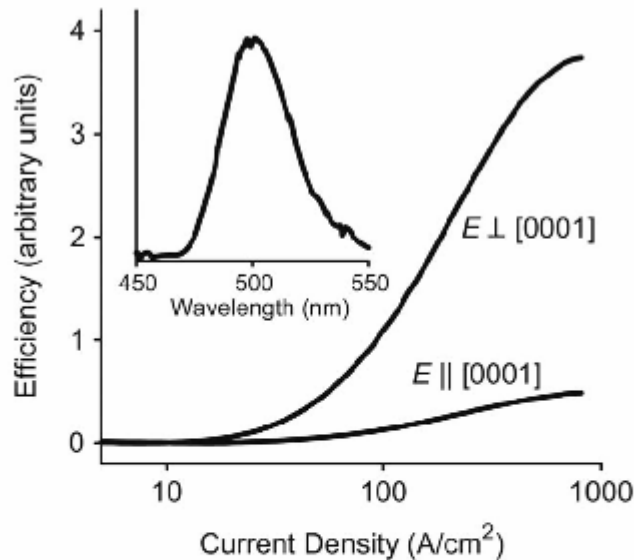


FIG. 4. Electroluminescence efficiency of the *m* plane InGaN LED as a function of current density, with a wire-grid polarizer placed between the sample and the photodetector selecting the polarization of the luminescence.  $E||[0001]$  indicates that the polarization is parallel to the *c* axis while  $E \perp [0001]$  indicates that the polarization is perpendicular to the *c* axis. The inset shows the electroluminescence spectrum at 500 A/cm<sup>2</sup> (both polarizations of light are included).

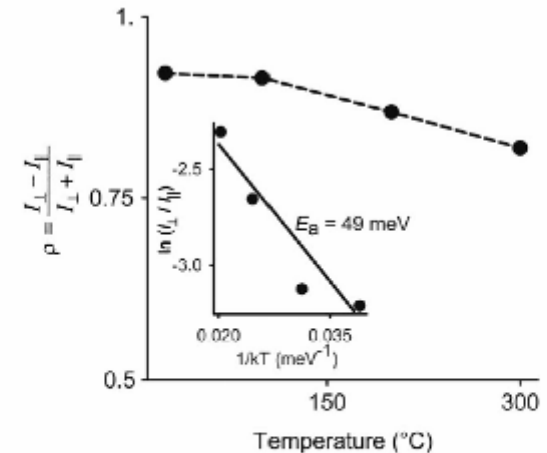


FIG. 5. Polarization ratio of the *m* plane InGaN LED photoluminescence as temperature is increased from room temperature to 300 °C. The polarization ratio is defined relative to the *c* axis. The inset shows the data plotted in an Arrhenius relationship with a fitted activation energy of 49 meV.

# Advantages of N-face GaN for HEMTs

- Low gate leakage [1,2,3]
- Low contact resistance [1,2,3]
- Enhancement mode operation [1,2,3]
- Enhanced back barrier confinement [1,2,3]
- InN channel [4]

[1] S. Rajan *et al.*, Jpn. J. Appl. Phys. **44** (2005) L1178.

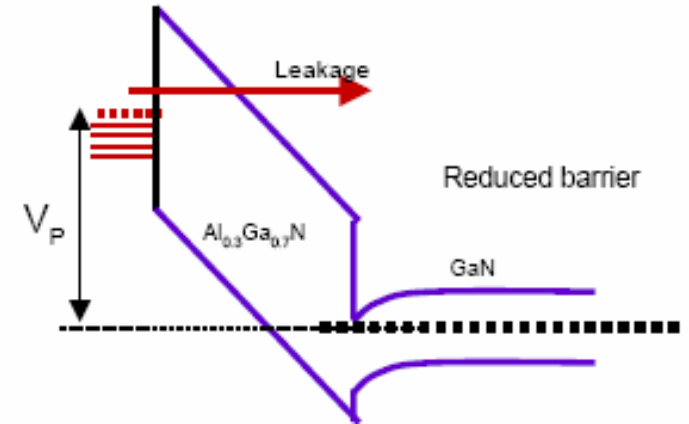
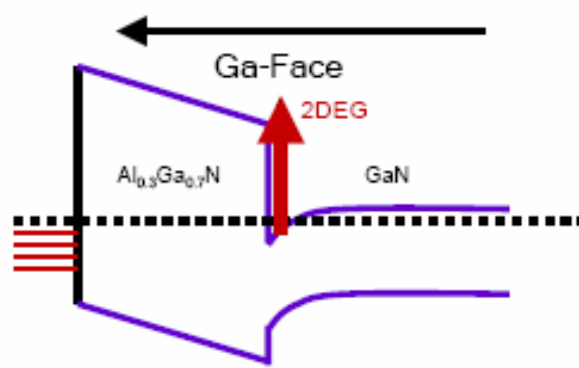
[2] S. Rajan *et al.*, 32<sup>nd</sup> International Symposium on Compound Semiconductors (ISCS), Sept 18-22 (2005), Europa- Park Rust, Germany

[3] S. Rajan, Ph.D. Thesis, University of California at Santa Barbara (2006).

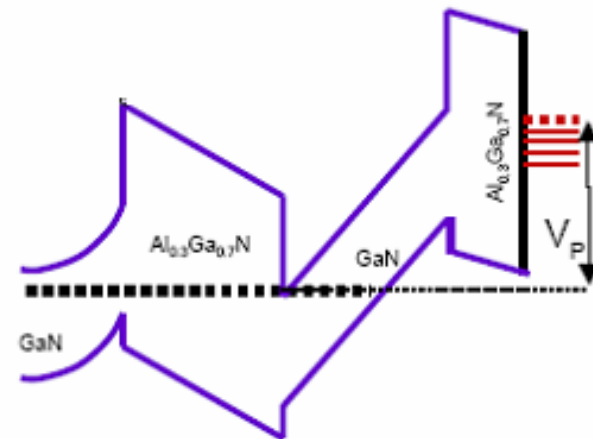
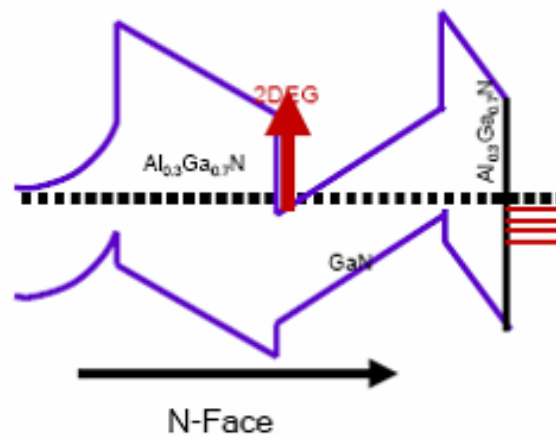
[4] K. Xu *et al.*, Appl. Phys. Lett. **83**, 251 (2003).

# Advantages of N-Face GaN for HEMTs

Ga-face



N-face



# Outline

---

## **Background on GaN symmetry and properties**

Crystal symmetry

Physical properties: heterostructures

## **A-plane and M-plane growth**

Common Microstructure

Defect reduction

Doping

Devices

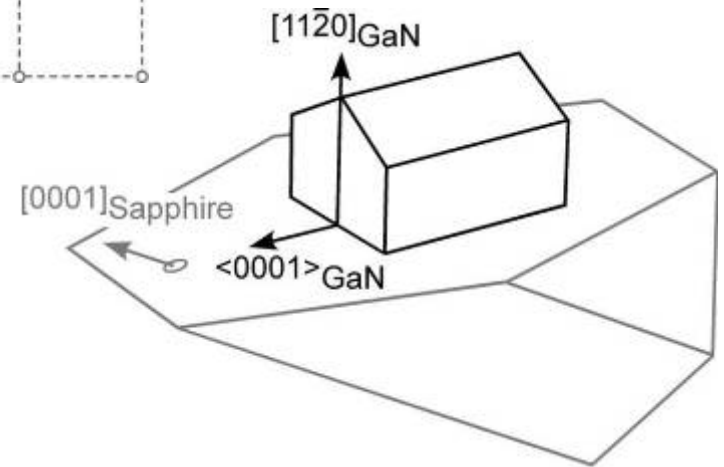
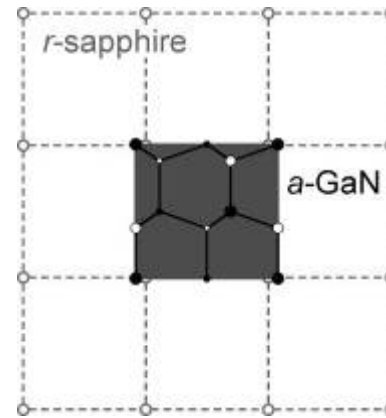
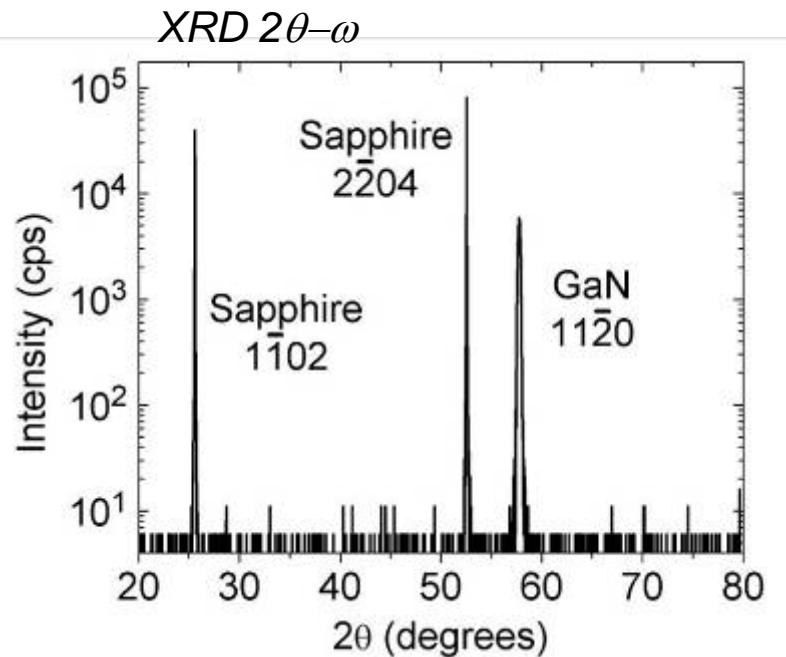
## **Semi-polar GaN**

New orientations and possibilities

## **N-face GaN**

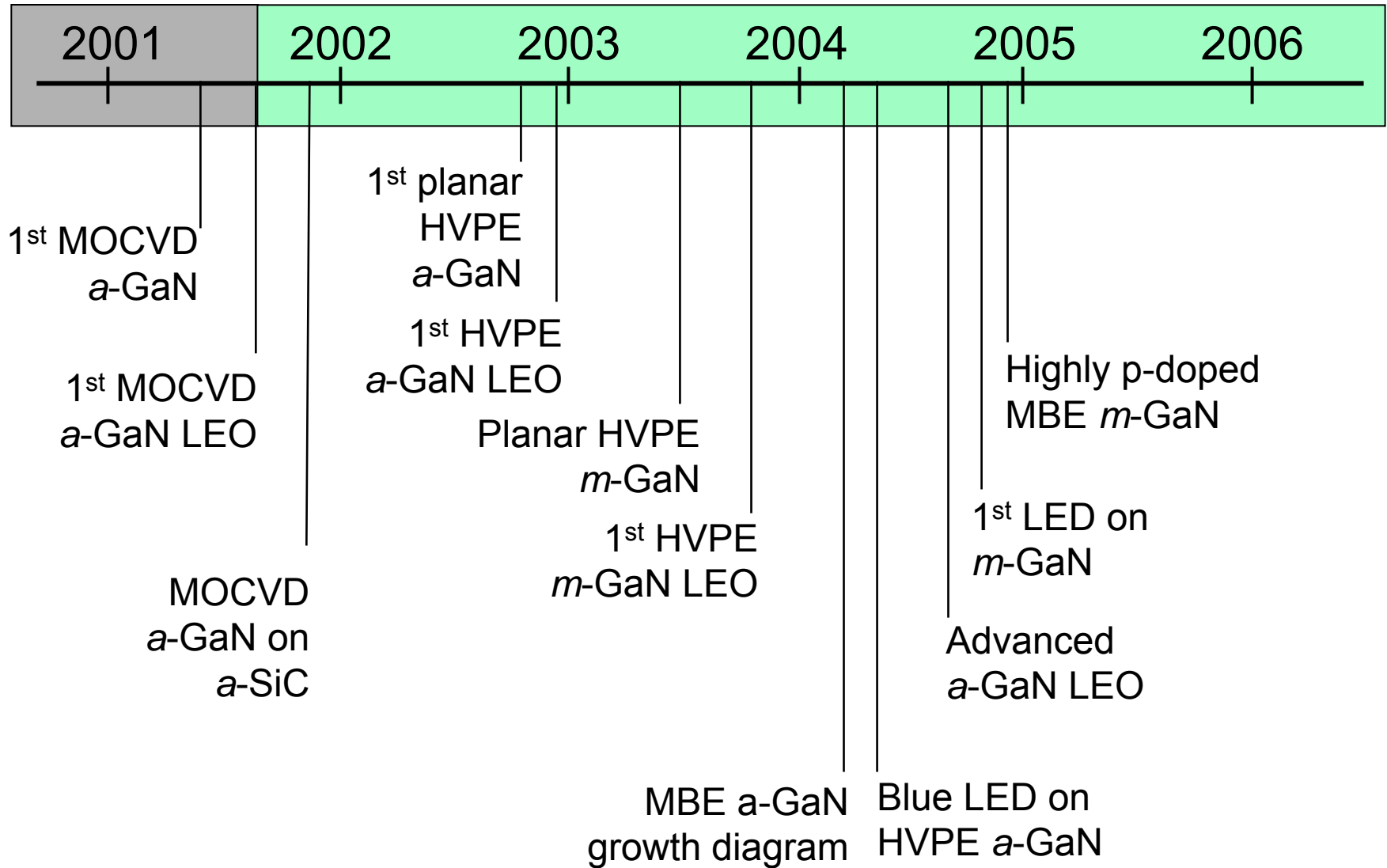
Turning the crystal and devices upside down ...

# Epitaxial Relationship

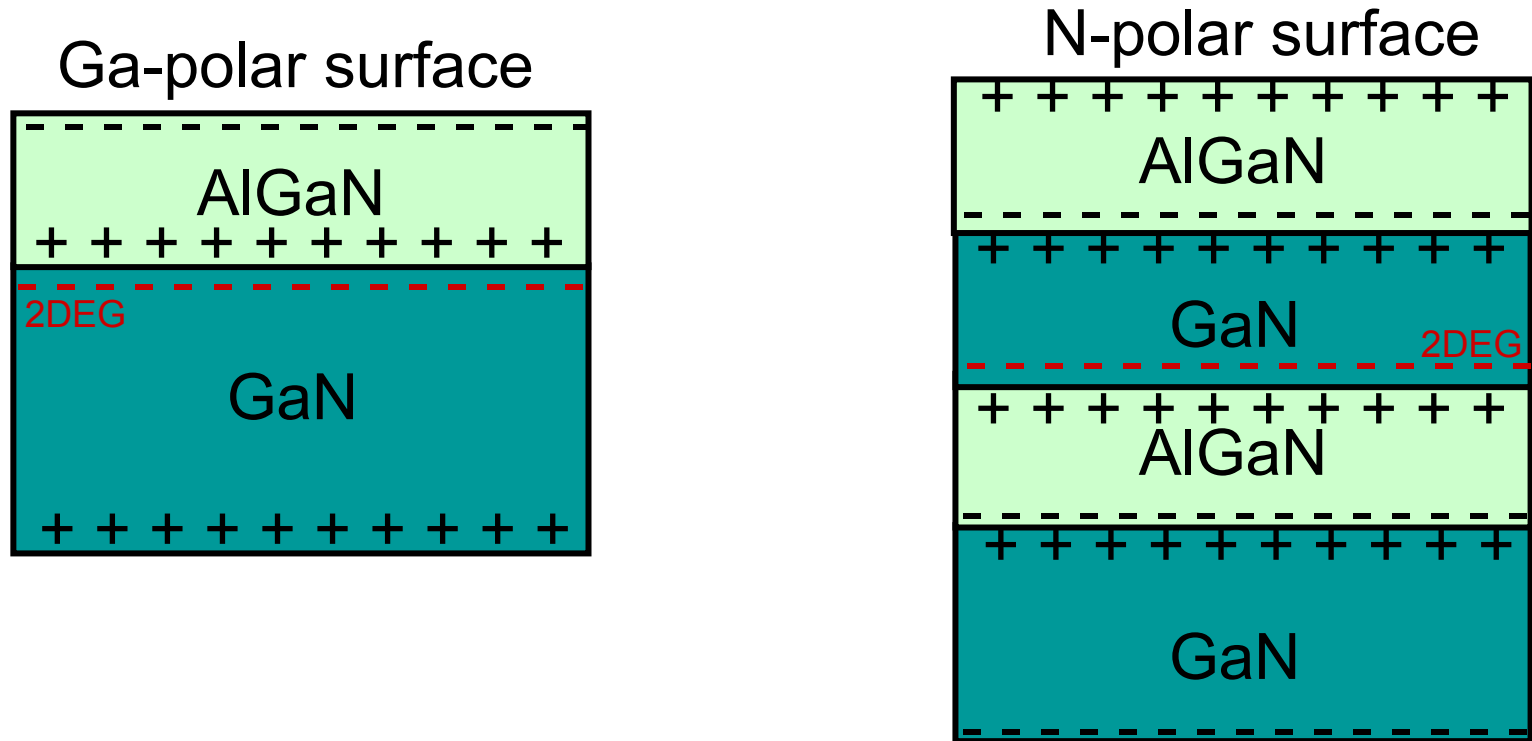


- *a*-GaN ( $11\bar{2}0$ ) growth surface
- GaN *c*-axis aligns with sapphire *c*-axis projection
  - Convergent beam electron diffraction (CBED) determined polarity

# Research accomplishments – Non-polar GaN



# AlGaN/GaN Heterostructures



- N-face HEMT demonstrated promising performance
  - 2DEG in excess of  $10^{13}$  cm<sup>-2</sup> with mobility of 1300 cm<sup>2</sup>/Vs [1]
  - $f_t$  and  $f_{max}$  of 12 GHz and 26 GHz respectively [2]

[1] S. Rajan *et al.*, 47<sup>th</sup> Electronic Materials Conference, June 2005, Santa Barbara, CA

[2] A. Chini *et al.*, 63<sup>rd</sup> Device Research Conference, Conference Digest pp. 63-64.

# Non-Polar – Common Microstructure

## Systems

- *a*-GaN / *r*-Al<sub>2</sub>O<sub>3</sub> (MOCVD, HVPE and MBE)
- *a*-GaN / *a*-SiC (MOCVD, MBE, MBE → HVPE)
- *m*-GaN / *m*-SiC (MOCVD and MBE, MBE → HVPE)
- *m*-GaN / (001) LiAlO<sub>2</sub> (HVPE, MBE → HVPE)

TD density (total):  $\sim 1 \times 10^{10} \text{ cm}^{-2}$

SF density (total):  $> 1 \times 10^5 \text{ cm}^{-1}$

SFs associated with exposed N face (000-1) during early growth

## Solutions

In situ/ex situ nanomasking

Lateral Epitaxial Overgrowth (LEO)

Two-step Lateral Epitaxial Overgrowth

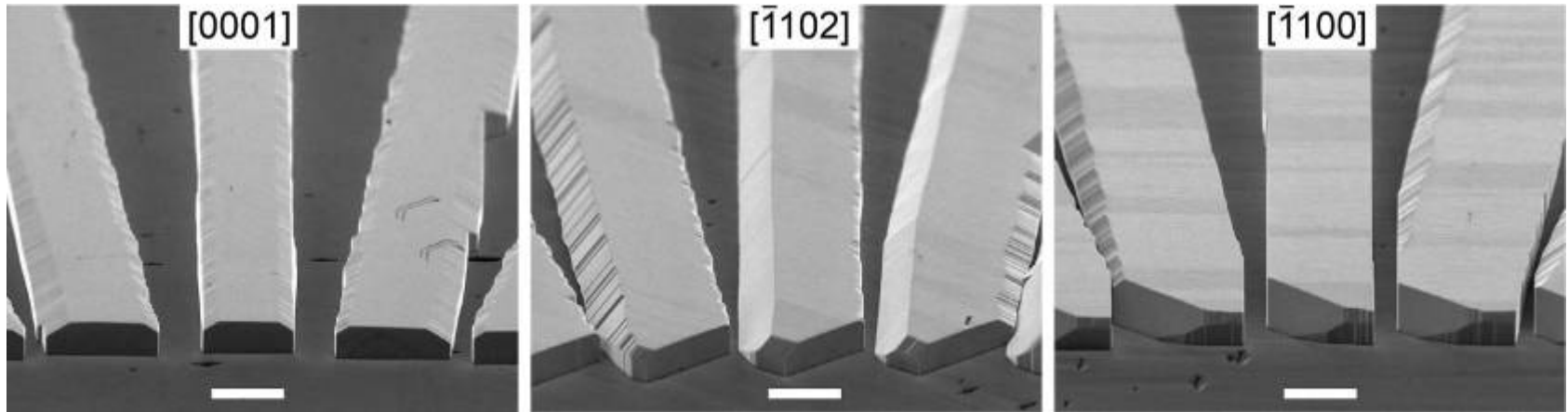
Sidewall LEO (SLEO)

'Bulk' GaN

# LEO Stripe Morphology

- Under the current LEO growth conditions...
  - [0001] symmetric stripe – mixture of vertical and inclined *m*-planes
  - $[\bar{1}102]$  asymmetric stripe – vertical and inclined sidewalls
  - $[\bar{1}100]$  **rectangular** x-sections with vertical *c*-plane sidewalls

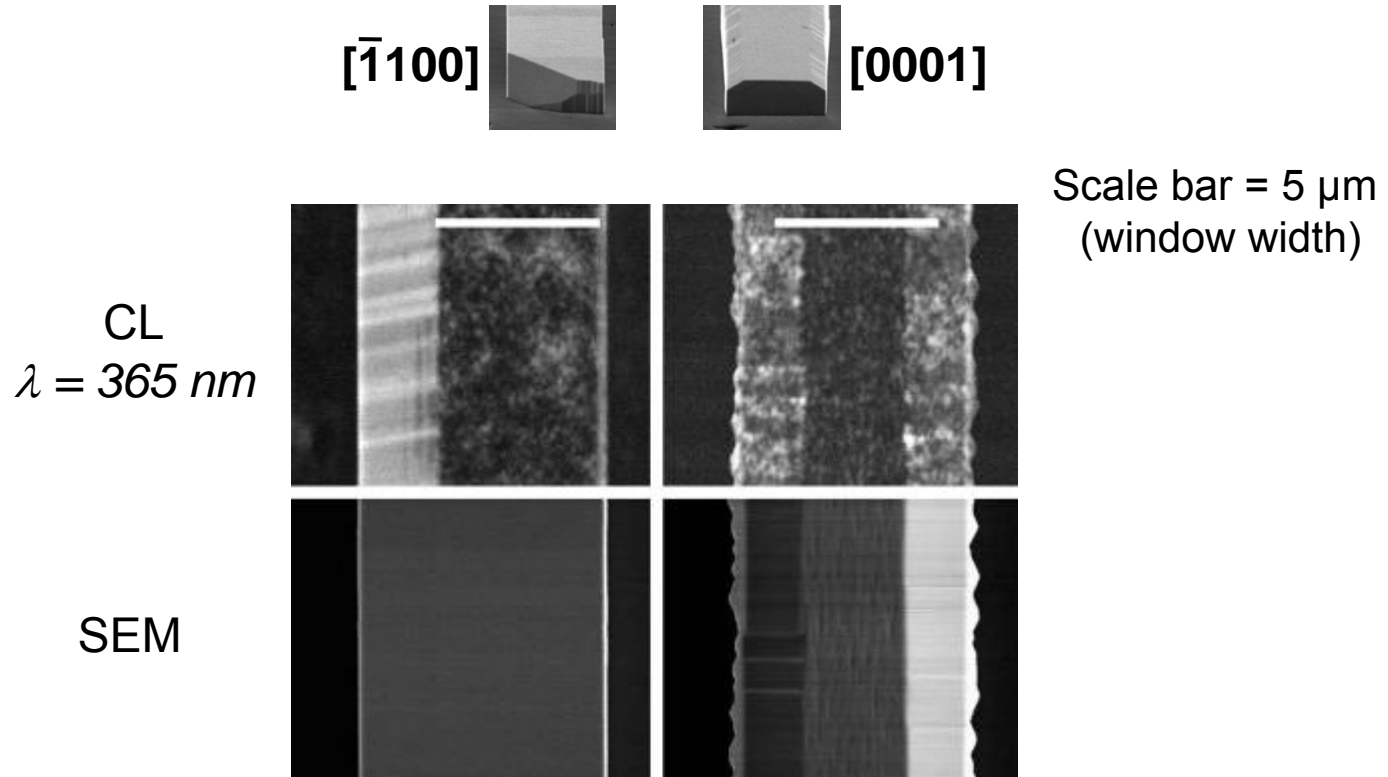
## *Inclined-view SEM*



Scale bar = 5  $\mu\text{m}$  (window width)



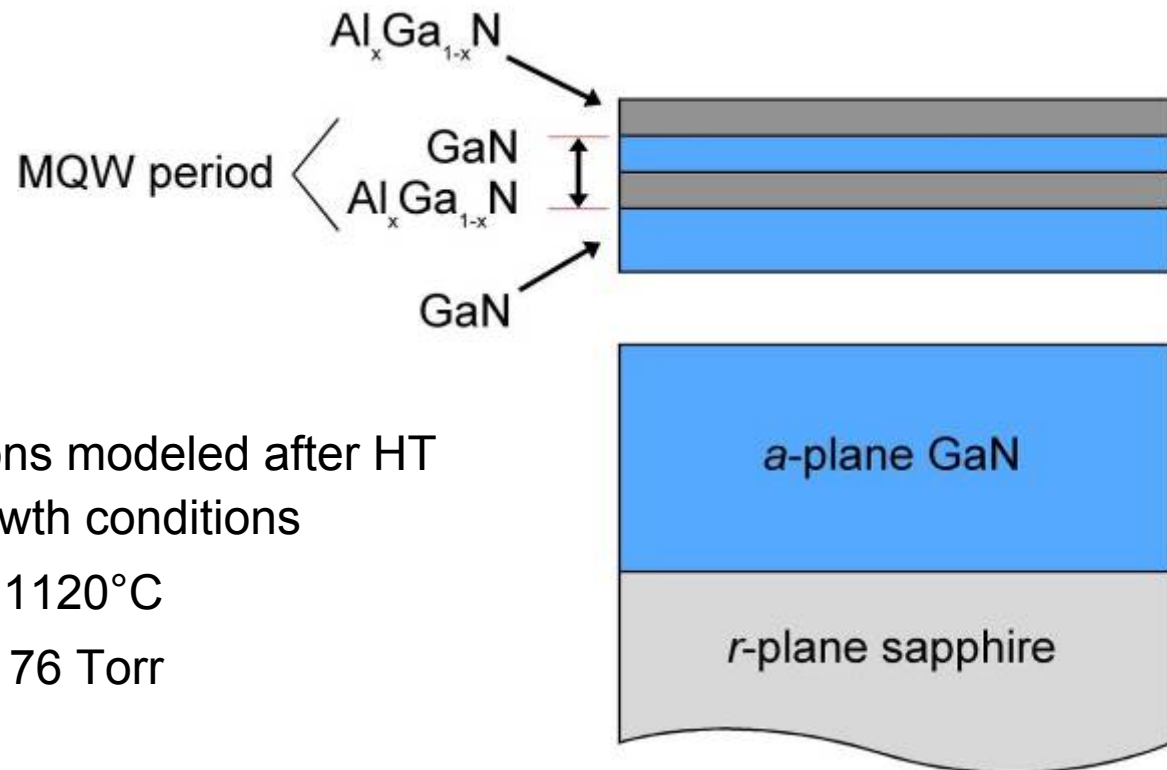
# Cathodoluminescence (CL)



- uniform luminescence from overgrowth of  $[1\bar{1}00]$  stripes
- 'mottling' extends across width of  $[0001]$  stripes

# *a*-plane GaN/AlGa<sub>x</sub>N MQWs

10-period GaN / Al<sub>x</sub>Ga<sub>1-x</sub>N MQWs regrown on *a*-GaN  
(and *c*-GaN) templates via MOCVD

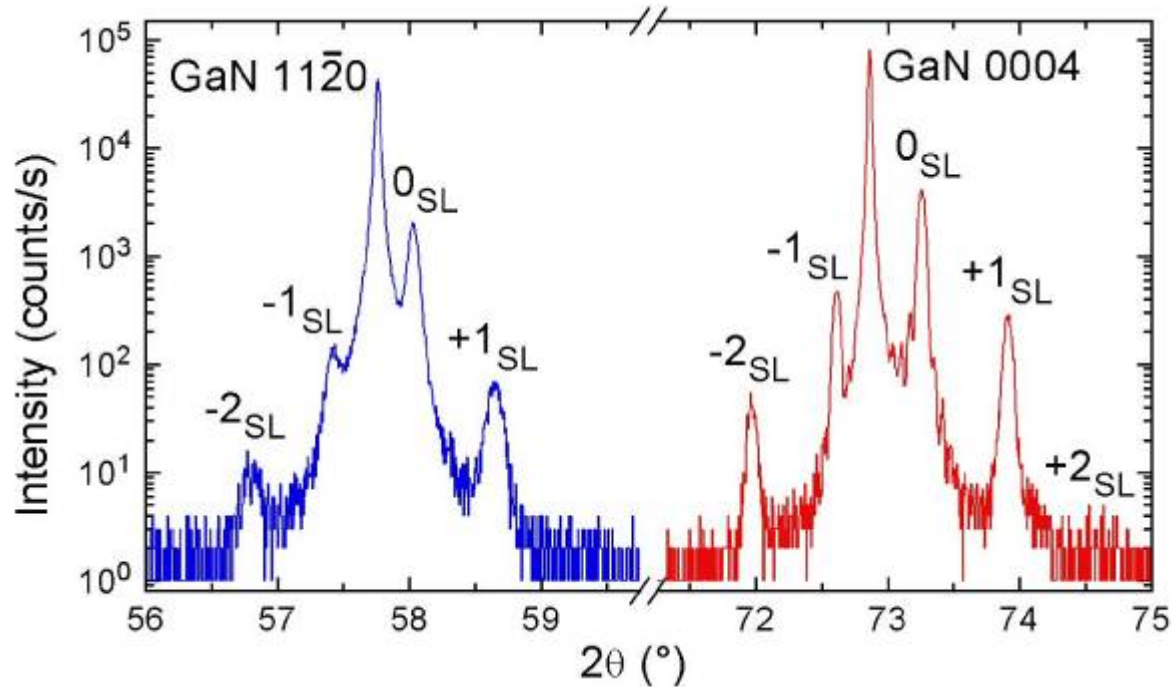


- Regrowth conditions modeled after HT epitaxial growth conditions
  - $T_{\text{growth}} \sim 1120^{\circ}\text{C}$
  - $P_{\text{reactor}} = 76 \text{ Torr}$

# a-plane vs. c-plane MQWs

- a- and c-plane MQWs *simultaneously* grown with varying well width

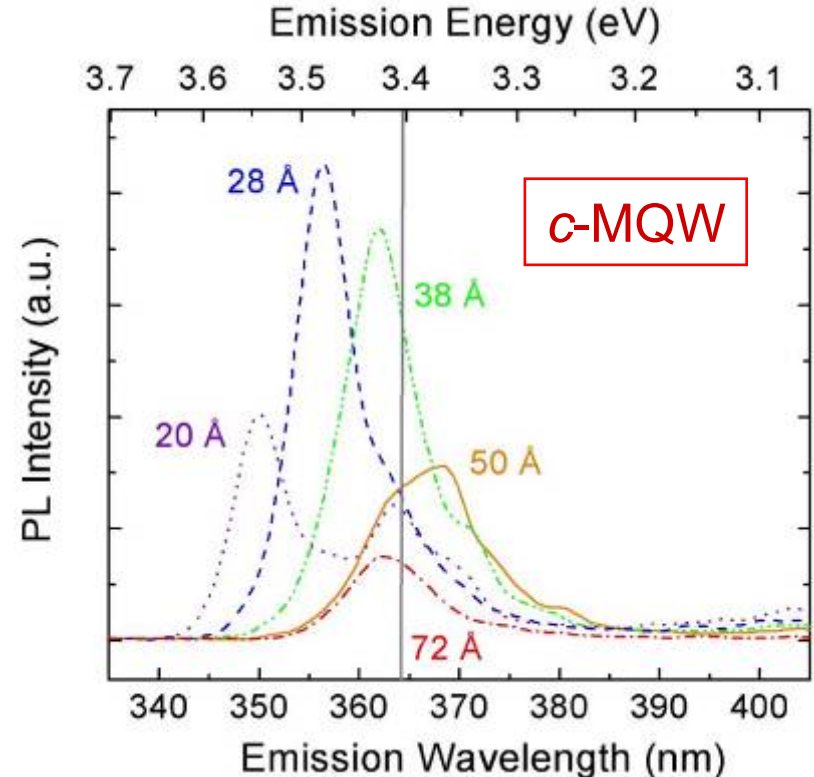
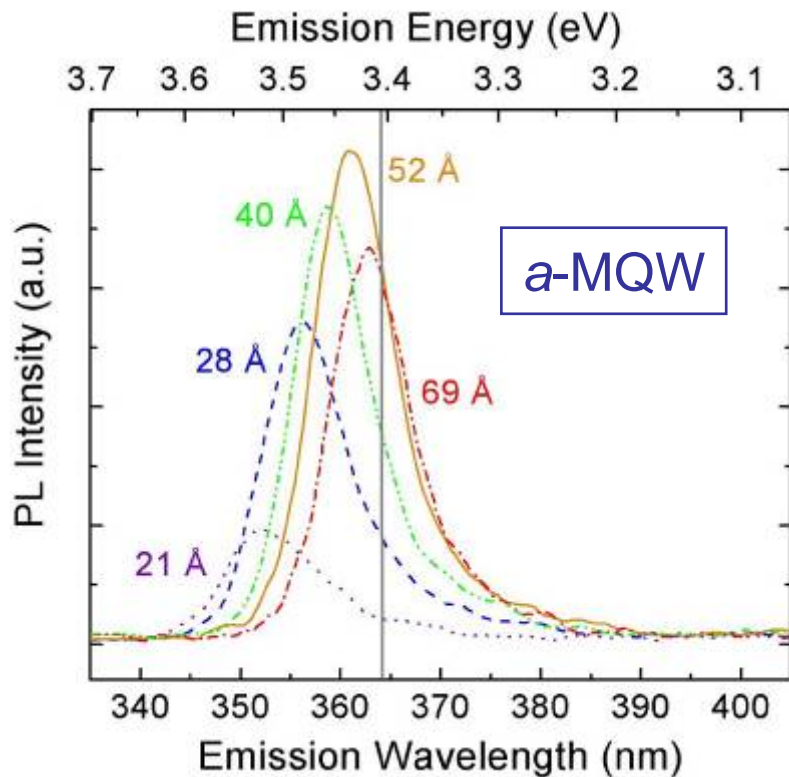
**a-plane**  
69Å GaN /  
96Å Al<sub>0.16</sub>GaN



**c-plane**  
72Å GaN /  
98Å Al<sub>0.16</sub>GaN

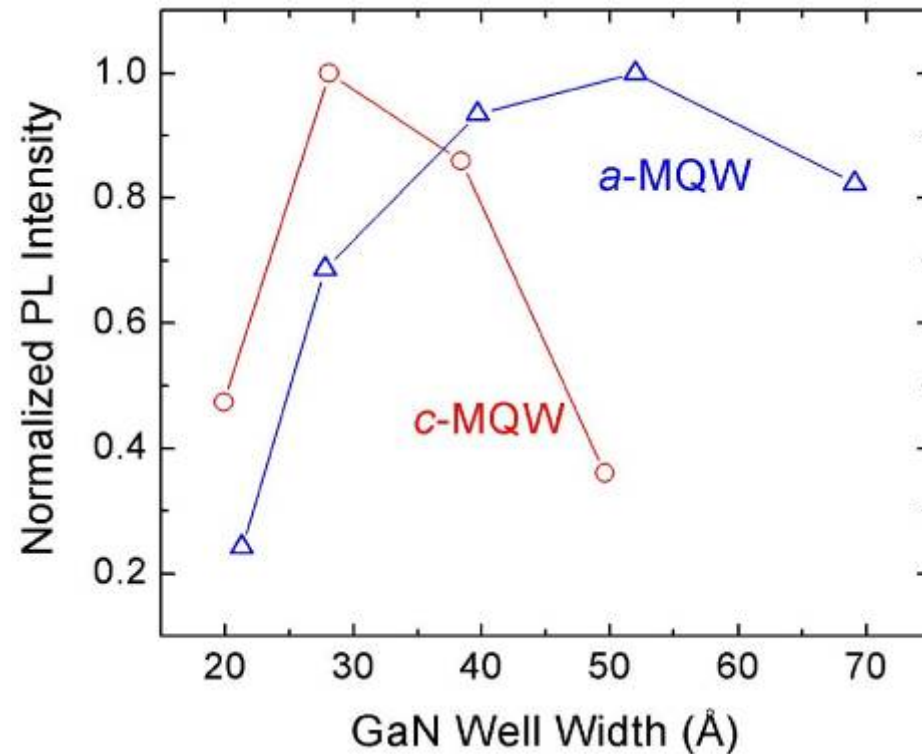
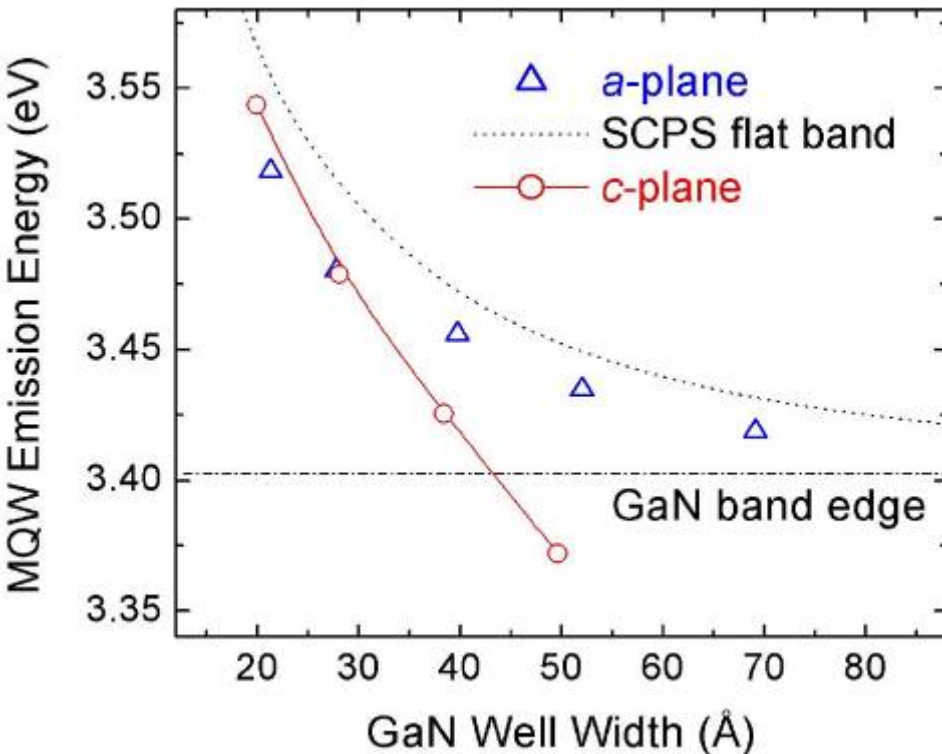
- a- and c-MQW dimensions and  $x_{\text{Al}}$  agree within 7%
- inferior a-MQW interface quality

# PL Emission vs. Well Width



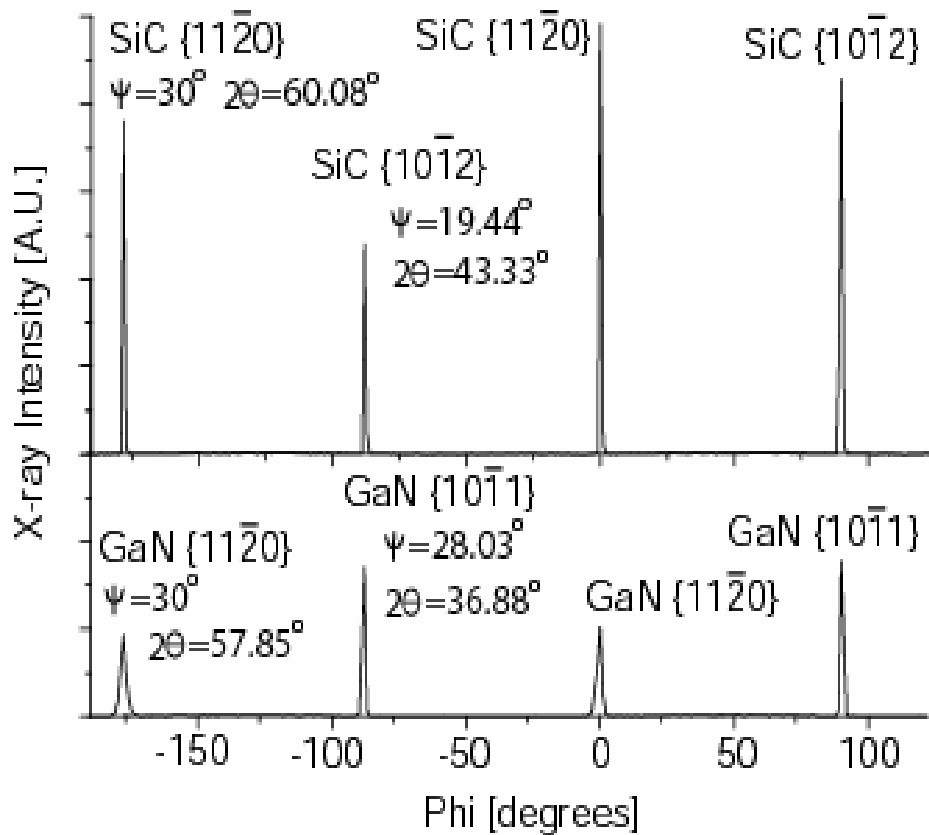
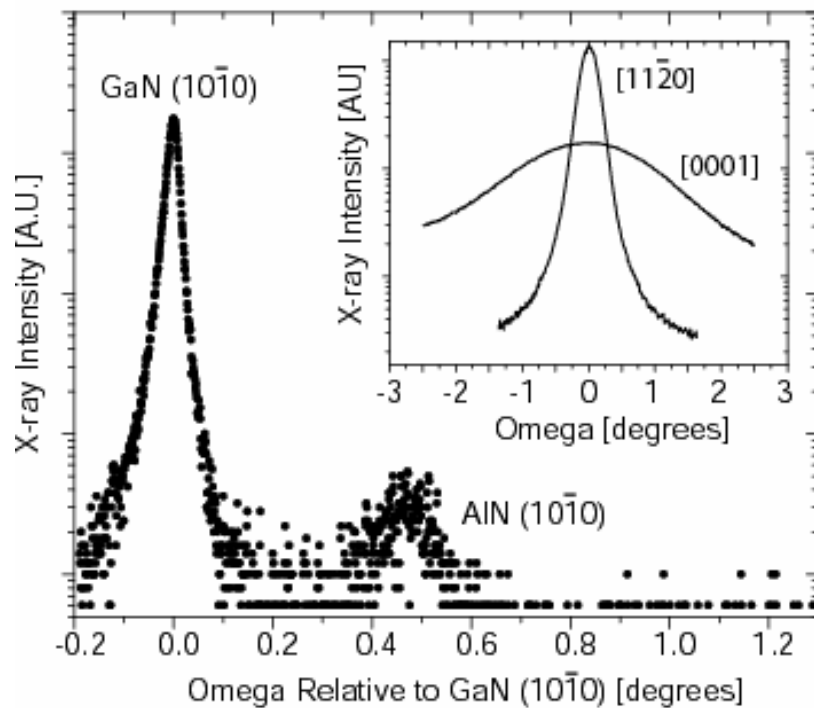
- MQW emission red-shifts with increasing GaN well width
  - a-plane: redshifts up to the GaN band edge
  - c-plane: redshifts **beyond** the GaN band edge

# MQW Emission Energy

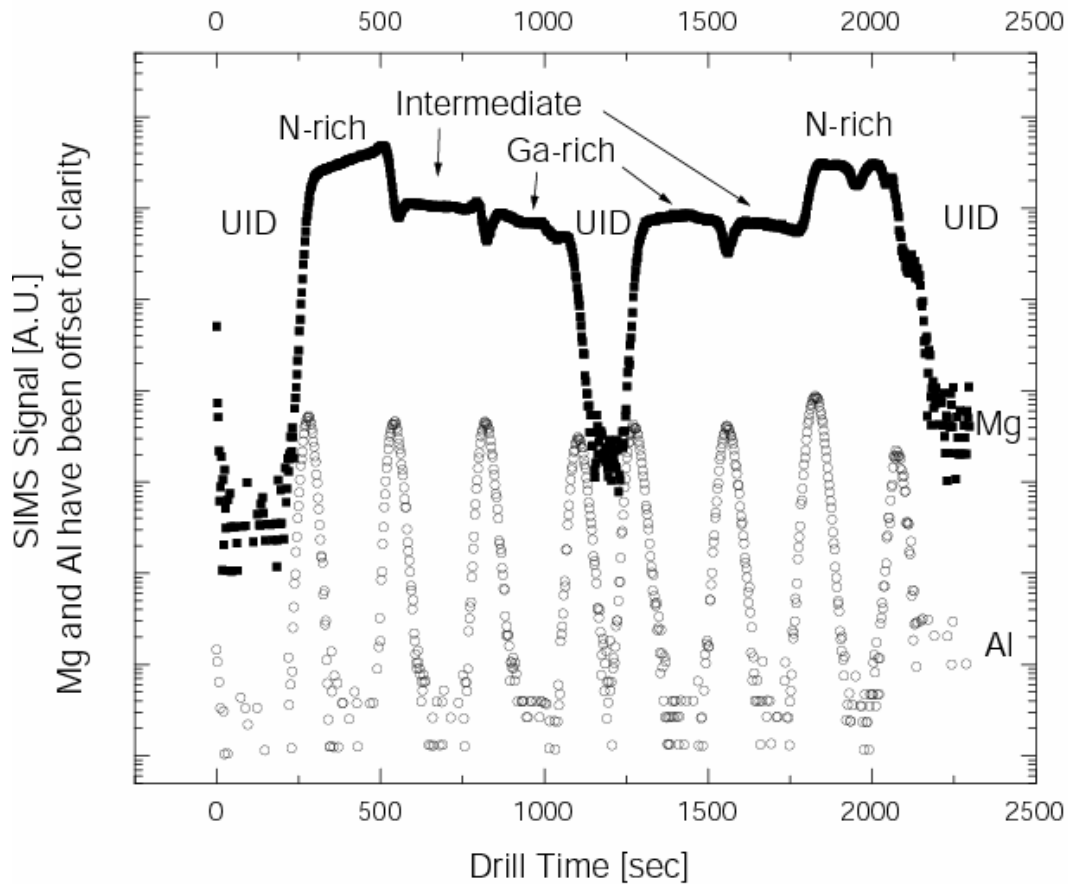


- a-MQW emission modeled using square well SCPS calculations
  - exciton binding energy accounts for model overestimation
  - ‘Nonpolar’ MQWs NOT Affected by Internal Electric Fields

# *m*-GaN on *m*-SiC: MBE



# *m*-GaN MBE: [Mg] vs. III-V Ratio



Substrate Temp ~ 530 °C on T.C.

## REGIME

Ga-rich

Intermediate

III/V = 1

N-rich

## Ga BEP [Torr]

3.3E-7

2.4E-7

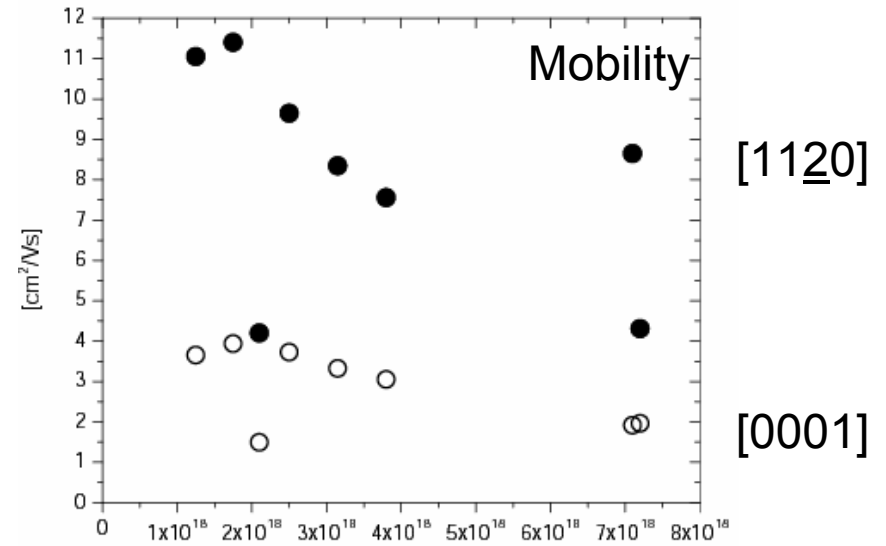
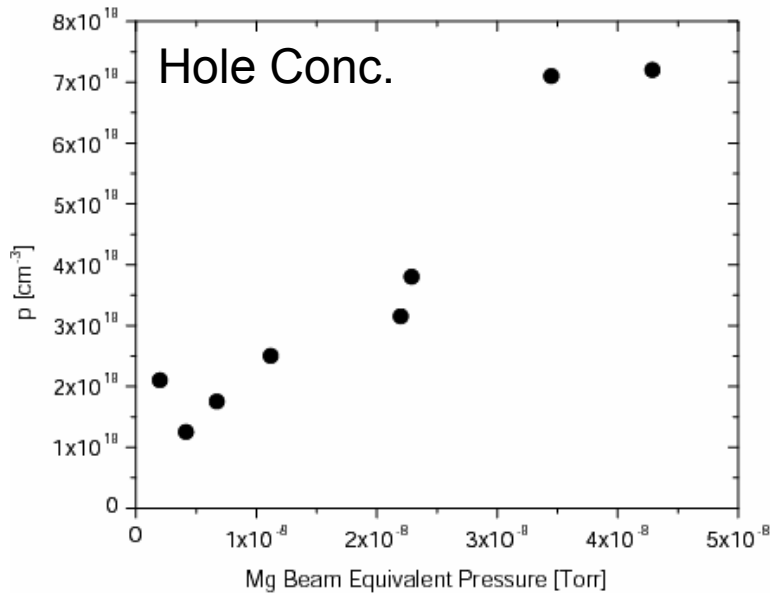
~2.26e-7

1.54E-7

Doped Layers ~100 nm thick

AlGaIn marker layers ~10 nm thick.

# 300K Transport Results



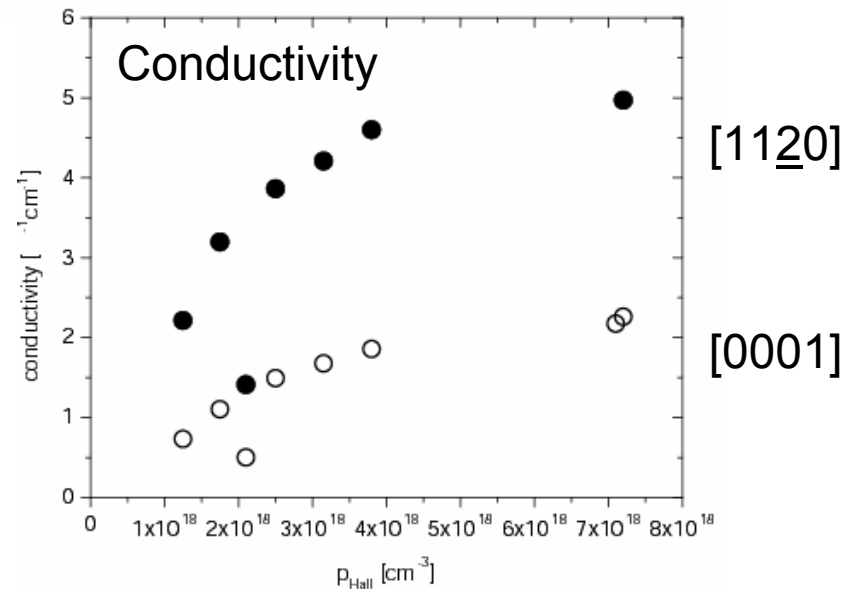
Carrier concentration: Hall bars // **a** and **c**

Conductivity: via TLM patterns // **a** and **c**

$$1 \times 10^{18} < p < 7 \times 10^{18} \text{ cm}^{-3}$$

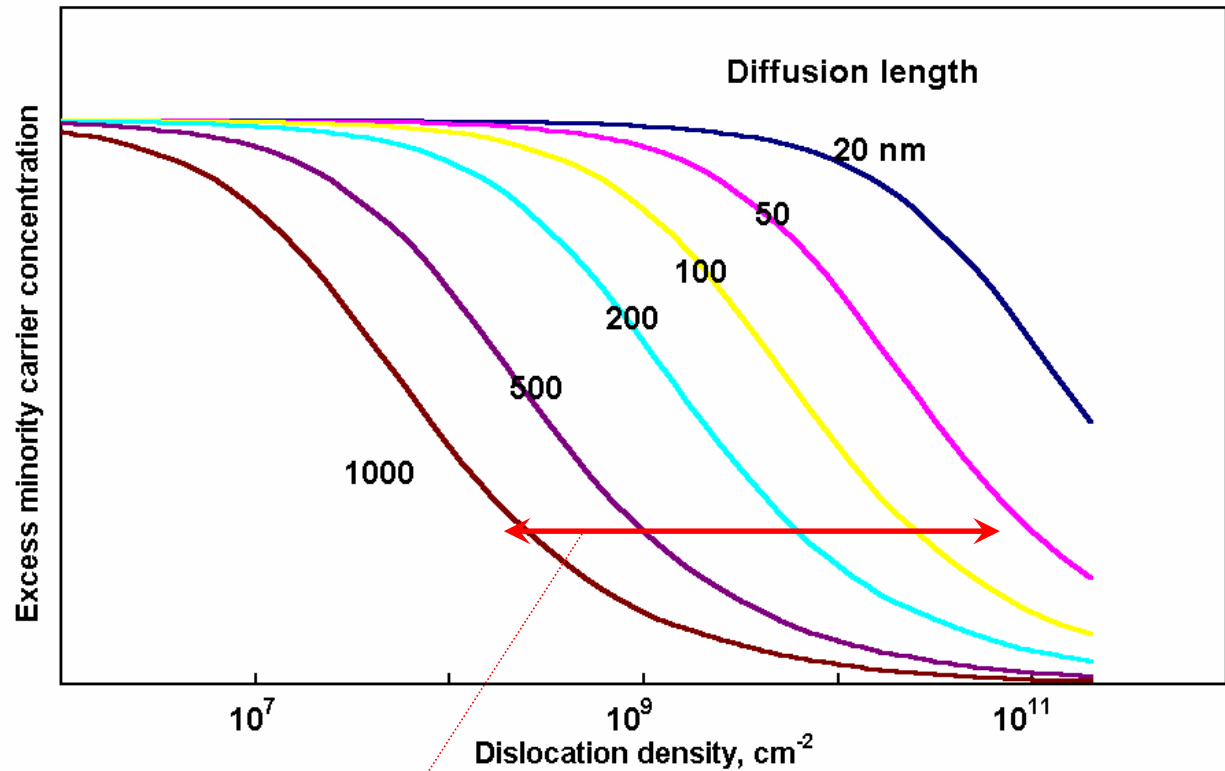
$$\mu \cdot p \uparrow \text{ as } p \uparrow \text{ to } p = 7 \times 10^{18} \text{ cm}^{-3}$$

Anisotropy in hole mobility: expected from anisotropic hole masses



# Excess Minority Carrier Concentration: Diffusion Length and Dislocation Density

*Luminescence intensity is proportional to excess minority carrier concentration.*



GaN: Minority carrier diffusion length:  $\sim 100$  nm (common)  
TDs are a limiting factor in non-polar LED performance

J.S. Speck and S.J. Rosner, *Physica B* **274**. 24 (1999)

## Nitride semiconductors free of electrostatic fields for efficient white light-emitting diodes

P. Waltereit, O. Brandt, A. Trampert, H. T. Grahn, J. Menniger, M. Ramsteiner, M. Reiche & K. H. Ploog

Paul-Drude-Institut für Festkörperelektronik, Hausvogteiplatz 5-7, D-10117 Berlin, Germany

Compact solid-state lamps based on light-emitting diodes (LEDs)<sup>1,2</sup> are of current technological interest as an alternative to conventional light bulbs. The brightest LEDs available so far emit red light and exhibit higher luminous efficiency than fluorescent lamps. If this luminous efficiency could be transferred to white LEDs, power consumption would be dramatically reduced, with great economic and ecological consequences. But the luminous efficiency of existing white LEDs is still very low, owing to the presence of electrostatic fields within the active layers<sup>3</sup>. These fields are generated by the spontaneous and piezoelectric polarization along the [0001] axis of hexagonal group-III nitrides—the commonly used materials for light generation<sup>4-6</sup>. Unfortunately, as this crystallographic orientation corresponds to the natural growth direction of these materials deposited on currently available substrates<sup>7</sup>. Here we demonstrate that the epitaxial growth of GaN/(Al,Ga)N on tetragonal LiAlO<sub>2</sub> in a non-polar direction allows the fabrication of structures free of electrostatic fields, resulting in an improved quantum efficiency. We expect that this approach will pave the way towards highly efficient white LEDs.

## letters to nature

NATURE | VOL 406 | 24 AUGUST 2000 | www.nature.com

*The first planar non-polar oriented wurtzite films ...*

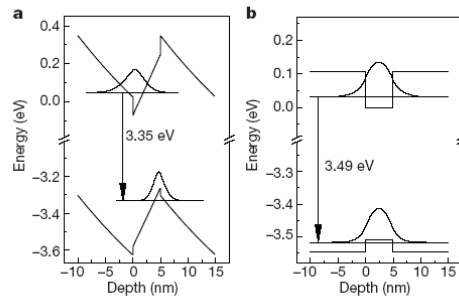
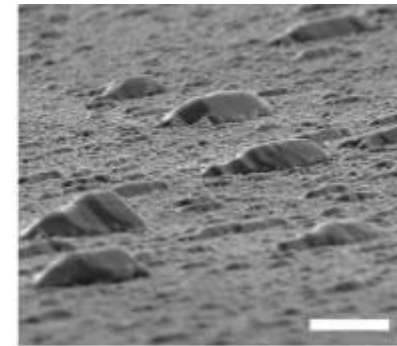
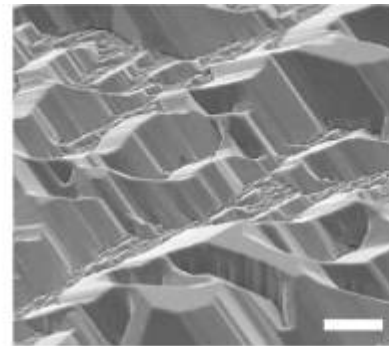
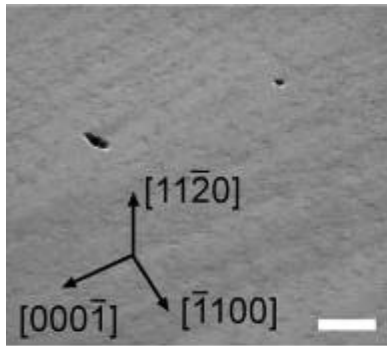


**Figure 1** Calculated band profiles in (5 nm GaN)/(10 nm Al<sub>0.1</sub>Ga<sub>0.9</sub>N) quantum wells. These profiles were obtained by self-consistent effective mass Schrödinger–Poisson calculations. The transition energies given take into account both strain and Coulomb interaction. **a**, The very large electrostatic fields in the [0001] orientation (polarization charges were taken from ref. 4) result in a quantum confined Stark effect and poor electron–hole overlap. **b**, The [1100] orientation is free of electrostatic fields, thus true flat-band conditions are established.

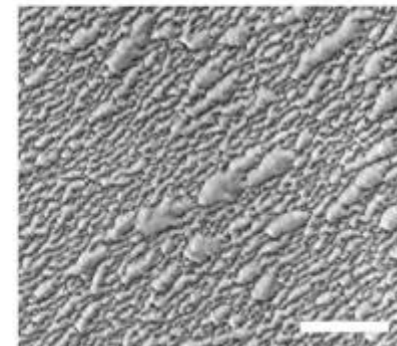
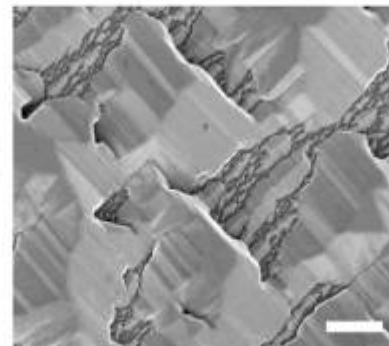
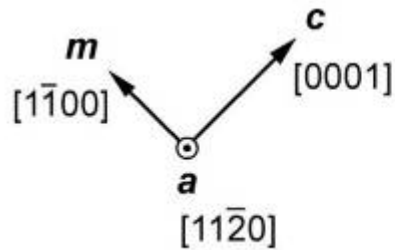
# Reactor Pressure - MOCVD

- Reactor Pressure: important growth variable

*inclined-view  
SEM*



*plan-view  
SEM*



76 Torr

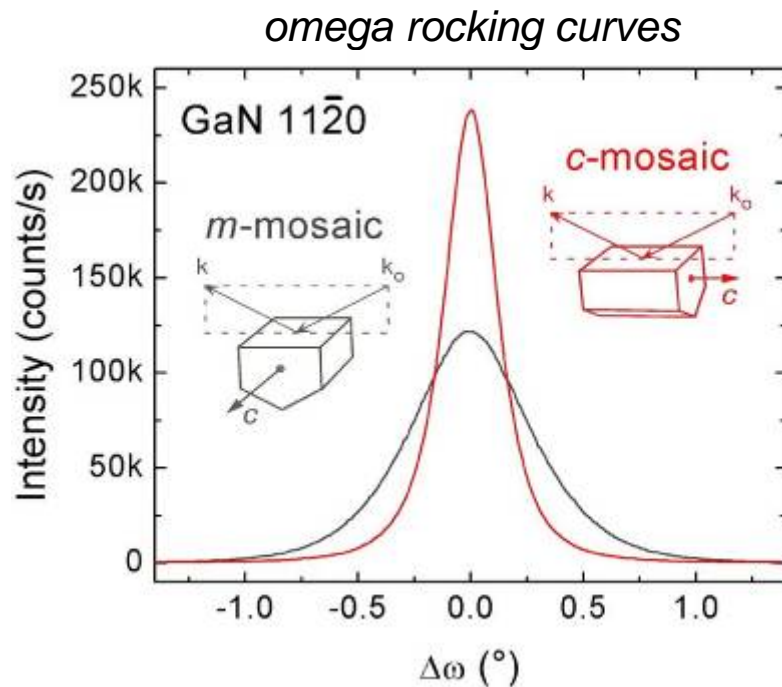
300 Torr

600 Torr

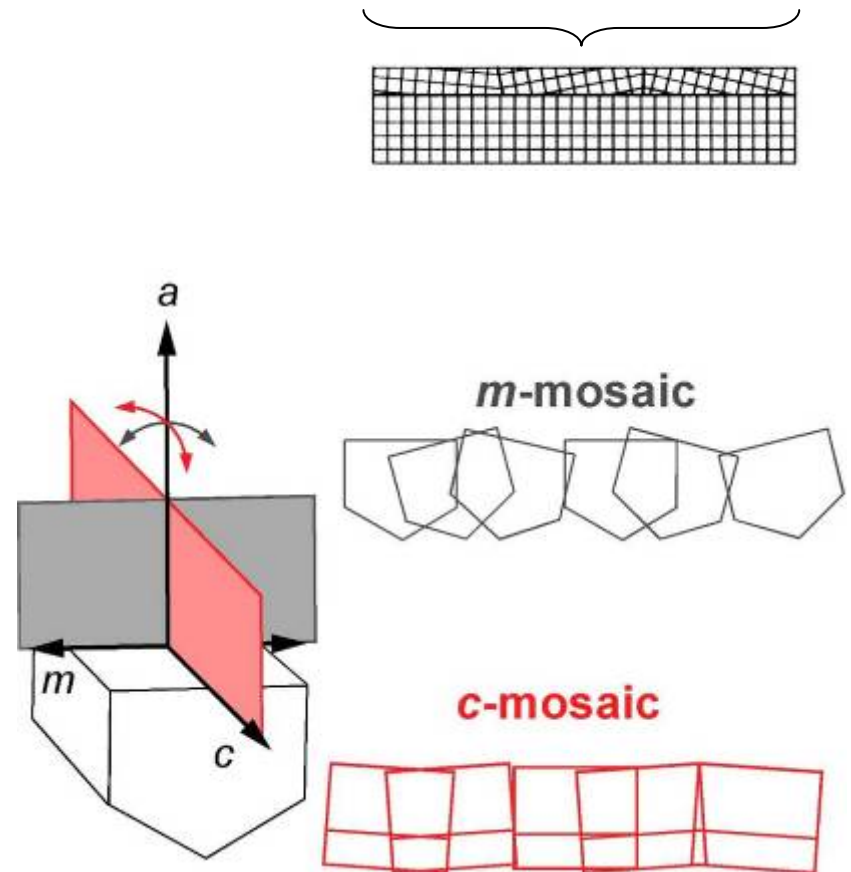
Reactor pressures  $\sim$ 76 Torr required for planar film growth

# Crystal Mosaic – a-GaN on r-Al<sub>2</sub>O<sub>3</sub>

- a-GaN on r-sapphire: orientation-dependent crystal tilt mosaic



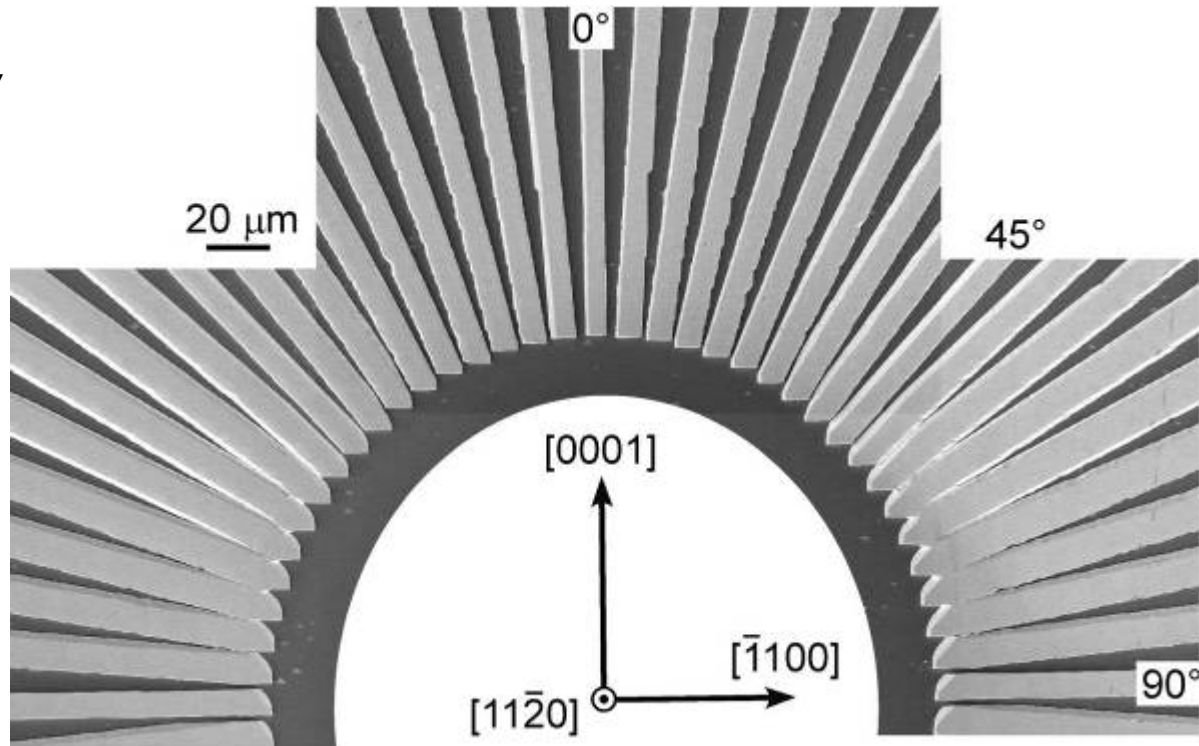
*c*-mosaic = 0.28° ( $\Delta c/c \sim 1.1\%$ )  
*m*-mosaic = 0.62° ( $\Delta a/a \sim 13.8\%$ )



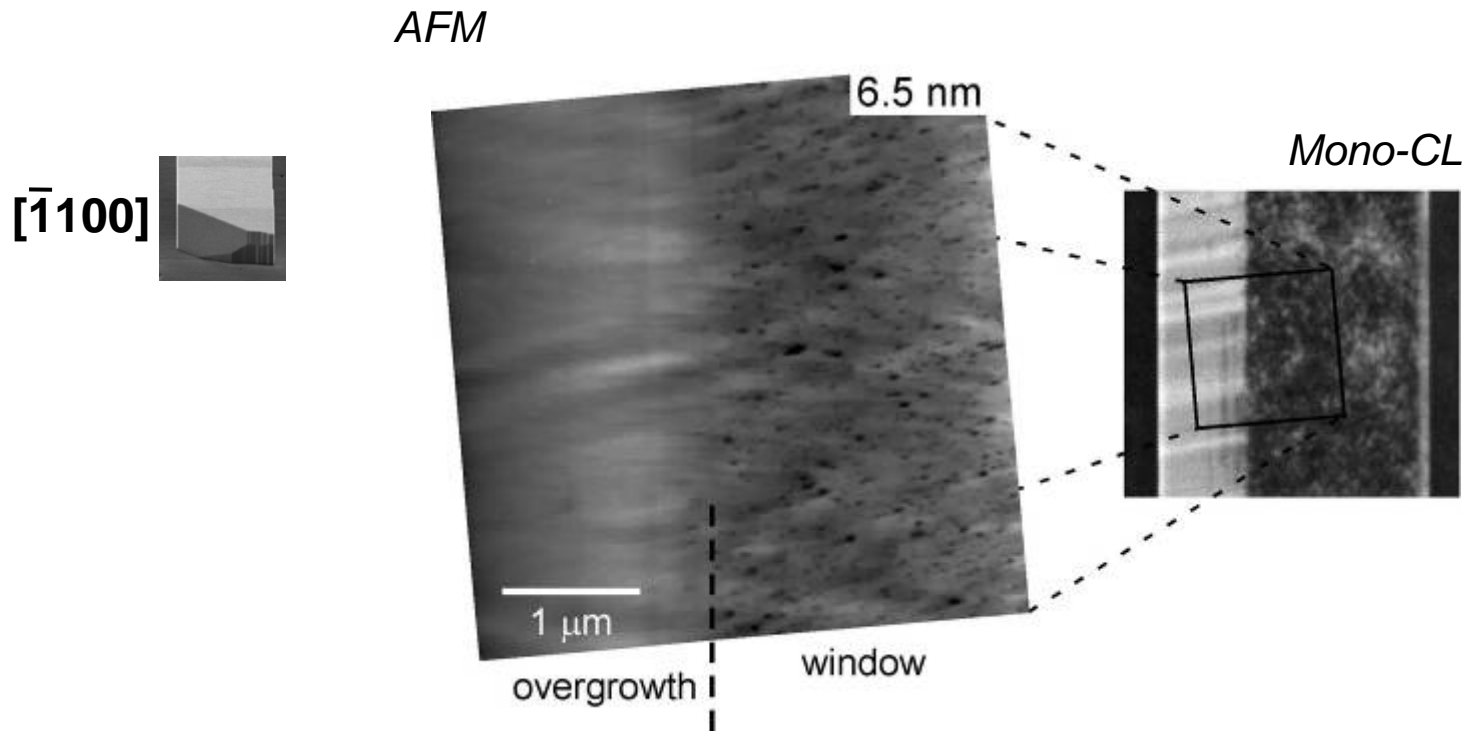
# LEO Orientation Analysis

- LEO stripe morphology dependent on stripe orientation
  - Analyzed using 'wagon wheel' mask
- Three primary orientations:  $[0001]$ ,  $[\bar{1}102]$ ,  $[\bar{1}100]$  ( $0^\circ$ ,  $45^\circ$ ,  $90^\circ$ )

*plan-view*  
**SEM**



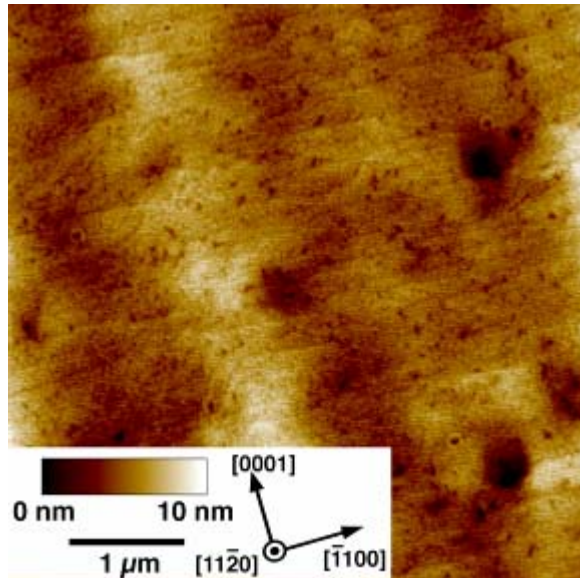
# Dislocation Reduction – AFM



- characteristic surface pits in window regions
- “pit-free” overgrowth
- *AFM pits decorate TD terminations*
- One-to-one pit-to-TD correspondence (AFM and TEM)

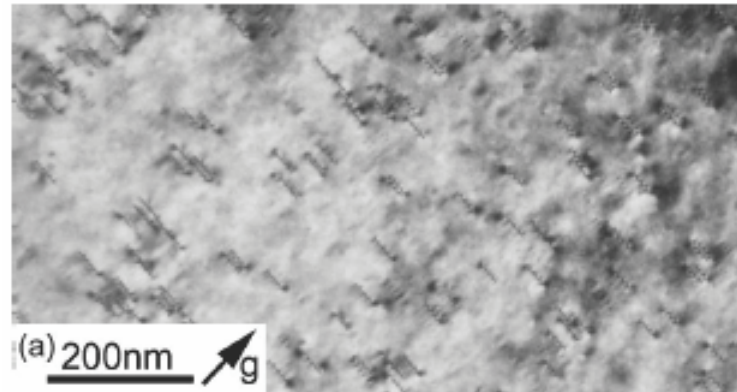
# Planar HVPE a-GaN

## AFM

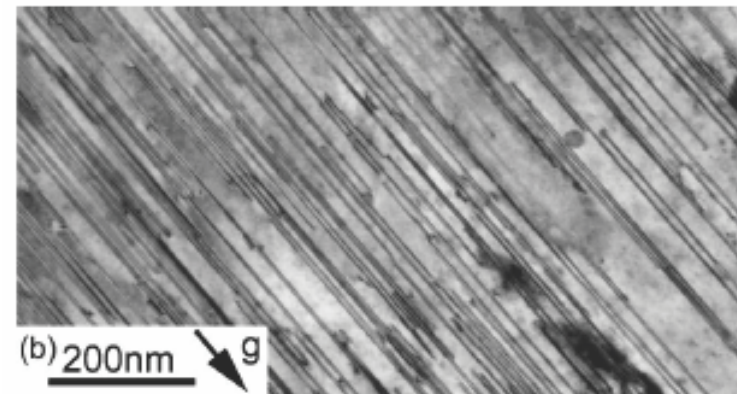


- Planar Surface decorated with high pit density.
- Faint ~1 nm steps oriented normal to  $\langle 0001 \rangle$ .
- RMS roughness ~1 nm.

## TEM



$g = 0002$



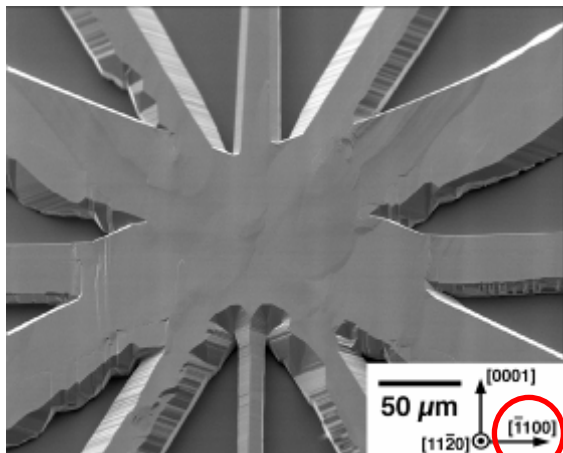
$g = 10\bar{1}0$

TDD:  $\sim 1 \times 10^{10} \text{ cm}^{-2}$

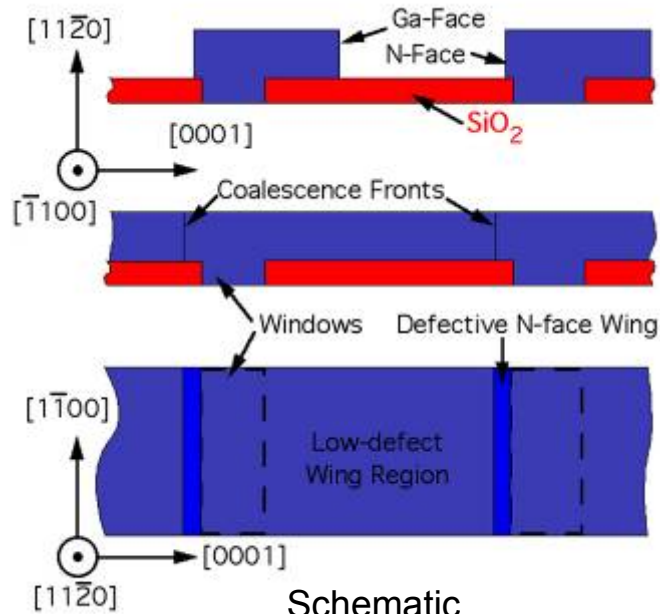
SFD:  $\sim 4 \times 10^5 \text{ cm}^{-1}$

Partial TDs:  $7 \times 10^9 \text{ cm}^{-2}$

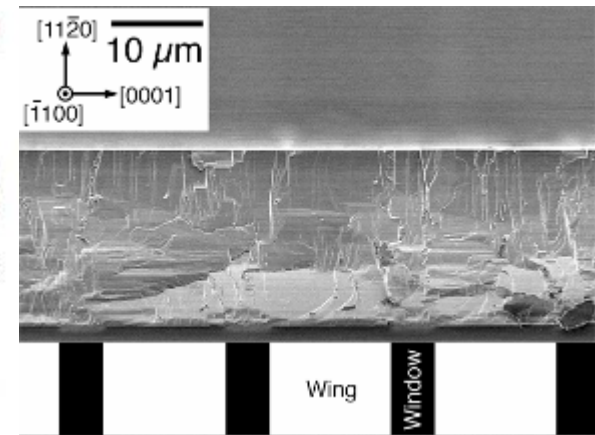
# HVPE LEO $\alpha$ -GaN



“Wagon Wheel” pattern



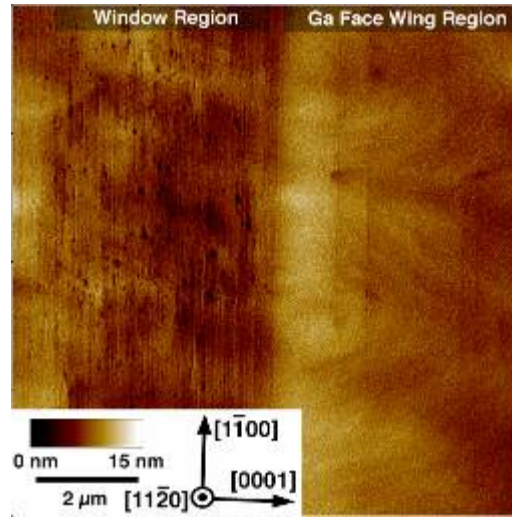
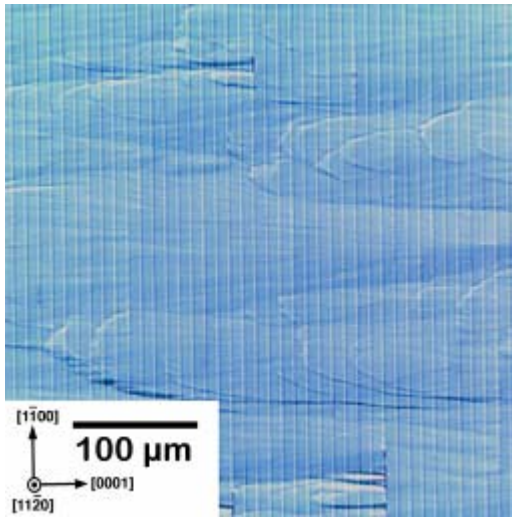
Schematic



Cross-Sectional SEM Image

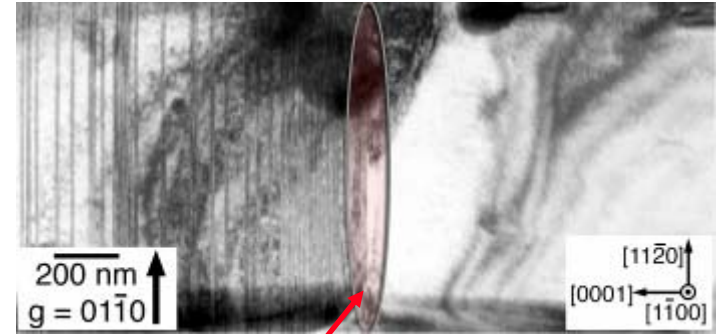
- $\langle 1\bar{1}00 \rangle$  stripes have vertical c-plane sidewalls.
- Ga-face (0001) lateral growth rate  $\sim 6\times$  N-face (000 $\bar{1}$ ) growth rate.
  - Coalescence front offset towards windows (large defect-free wing area results)

# HVPE LEO a-GaN (cont.)



N-Face Wing

Ga-Face Wing

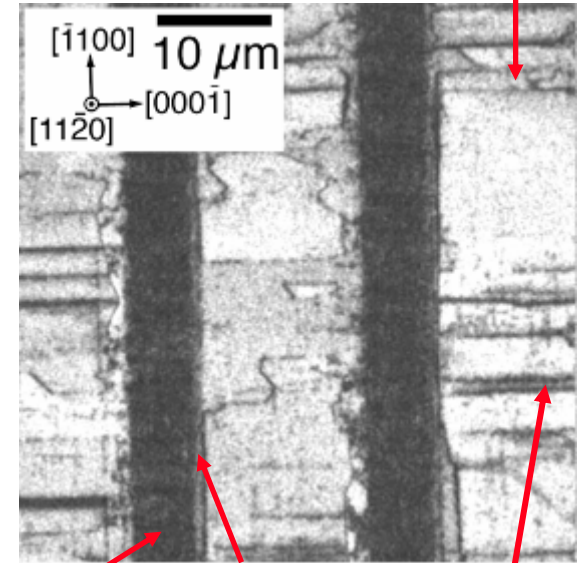


Coalescence Front

365 SEM Image

Ga-Face Wing

- Typical stripe patterns: 2 μm windows/8 μm wings (2/8), 5/5, and 5/15.
- Asymmetrical {0001} wing growth rates
- TDD of  $< 3 \times 10^{-6} \text{ cm}^{-2}$  and SFD of  $< 10^{-3} \text{ cm}^{-1}$  in wings; no measurable wing tilt.
- Four-fold increase in cathodoluminescence intensity in wings versus windows.



Window

N-Face Wing

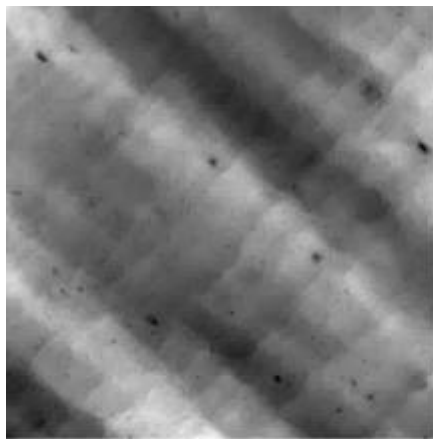
Inv. Domains

# *a*-GaN on *a*-SiC: Morphology & Orientation

➤ smooth *a*-GaN surface morphology

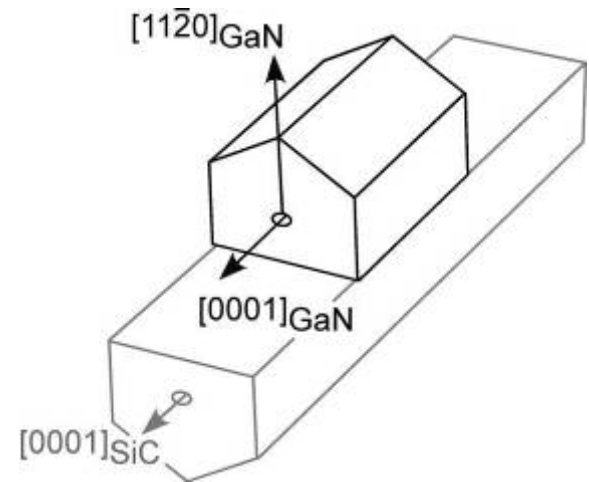
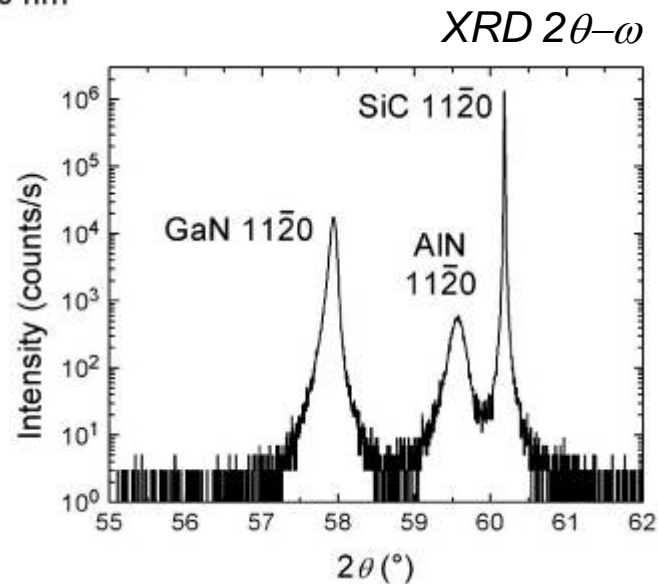
– *a*-AlN and *a*-GaN orientations match the *a*-SiC

AFM



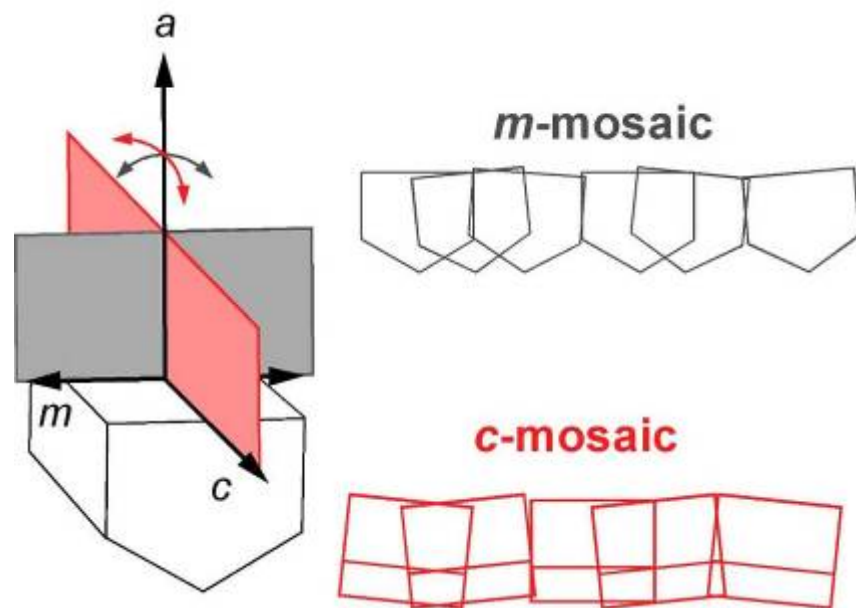
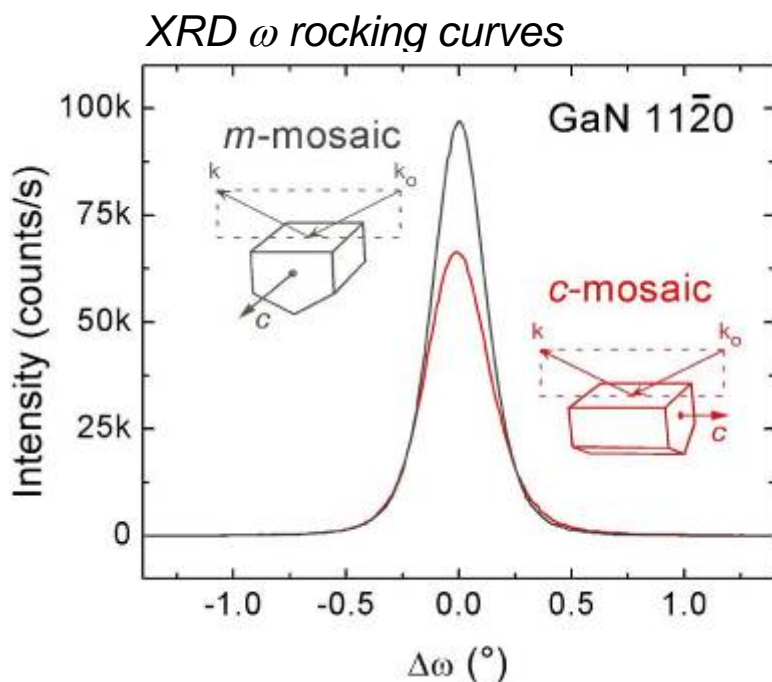
1 μm

14 nm  
0 nm



# *a*-GaN on *a*-SiC: Crystal Mosaic

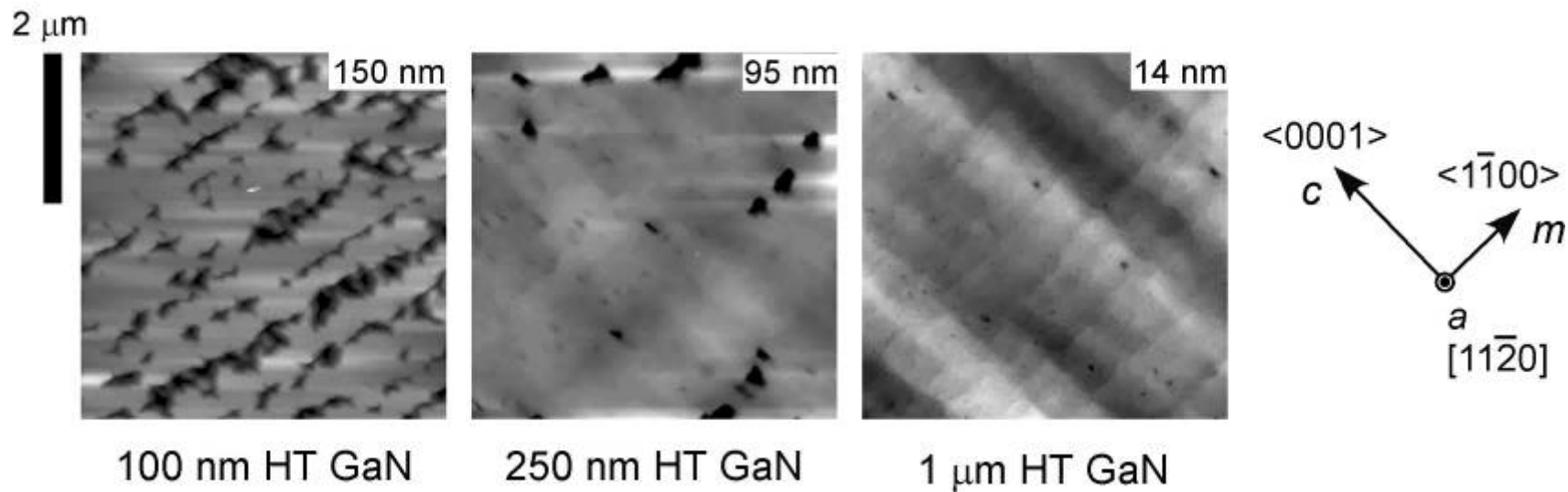
- Minimal tilt mosaic orientation dependence
  - *c*-mosaic greater than *m*-mosaic



*c*-mosaic =  $0.30^\circ$  ( $\Delta c/c \sim -2.8\%$ )  
*m*-mosaic =  $0.27^\circ$  ( $\Delta a/a \sim -3.4\%$ )

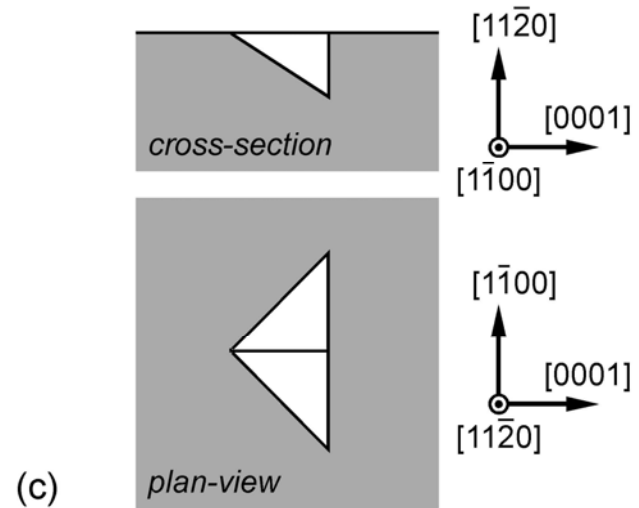
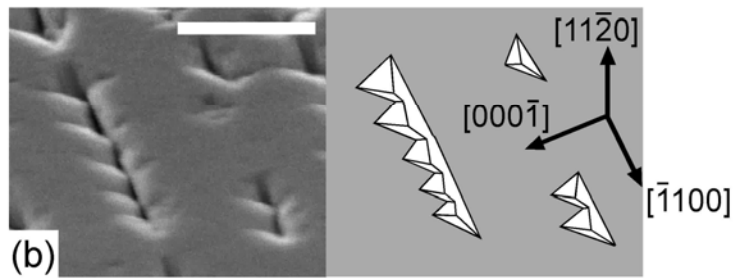
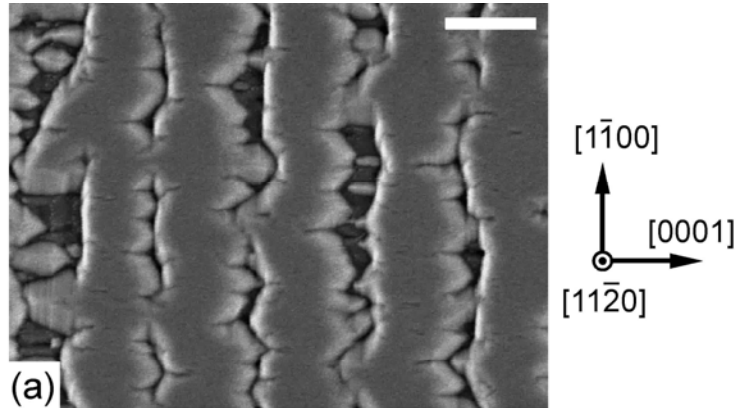
# *a*-GaN on *a*-SiC: Morphology

- *m*-Axis rows of coalesced GaN islands coalesce slowly along the *c*-axis
- Coalesced GaN surfaces feature:
  - Undulations along the *m*-axis
  - Low density of submicron pits
  - Crystallographic terraces perpendicular to *c*-axis



# $\alpha$ -GaN on $\alpha$ -SiC: N-face Surfaces

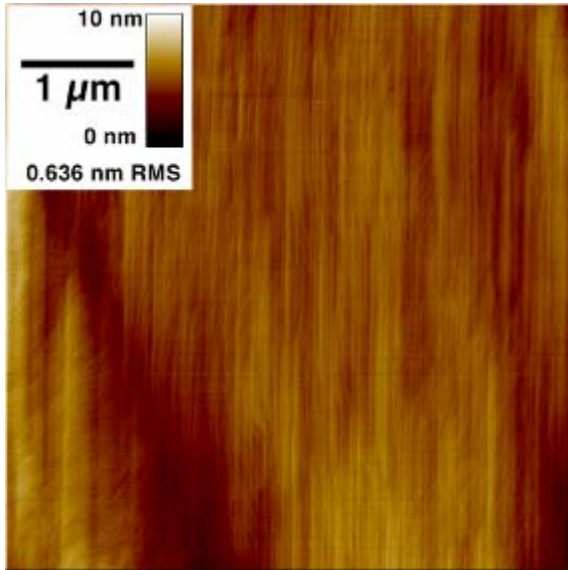
SEM – 100 nm GaN



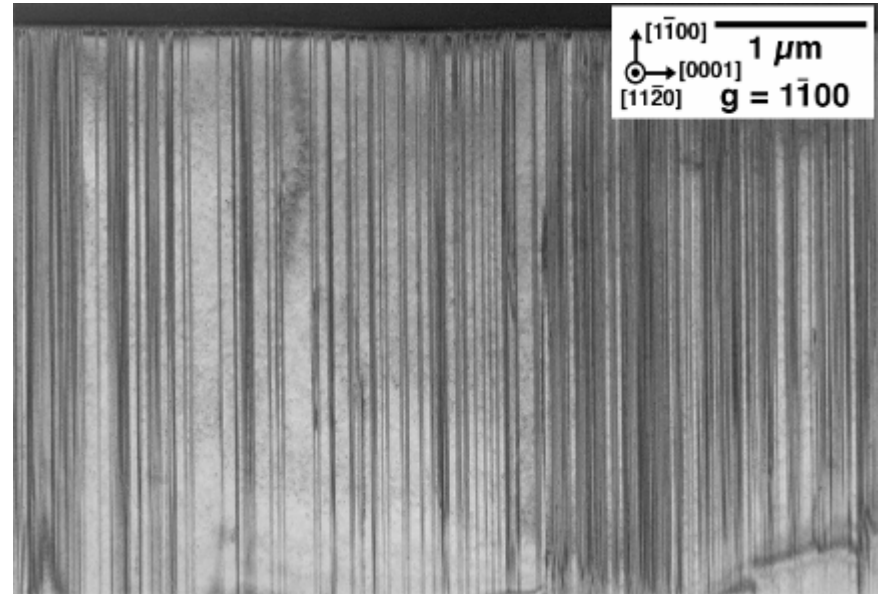
- Exposed N-face facets responsible for basal plane faulting

# Planar m-GaN (cont.)

## AFM

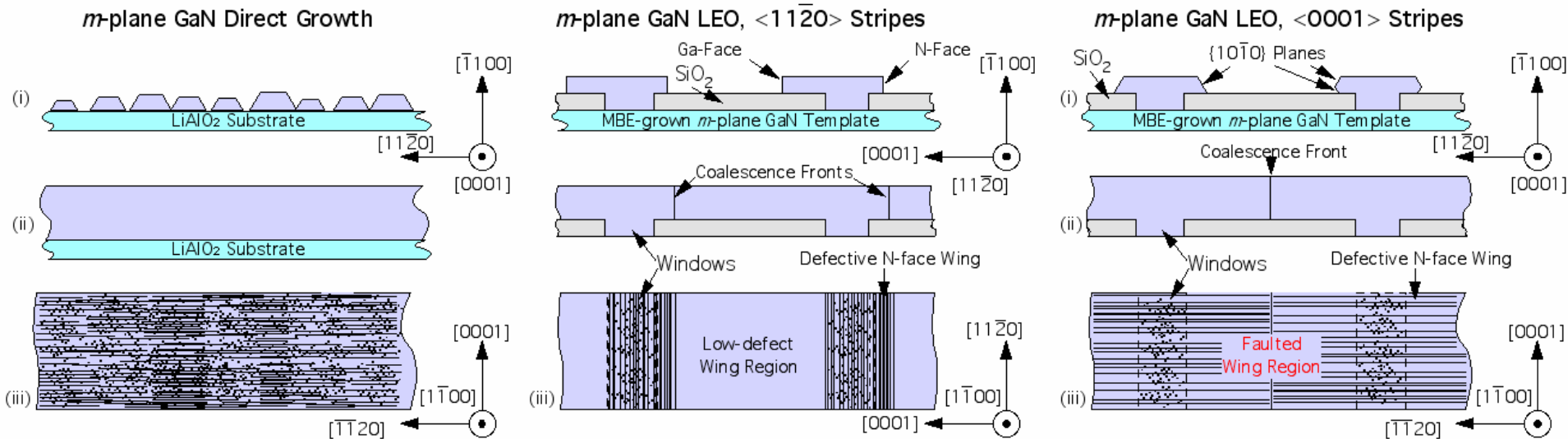


## TEM



- Threading dislocation density  $\sim 4 \times 10^9 \text{ cm}^{-2}$ .
- Basal plane stacking fault density  $\sim 1 \times 10^5 \text{ cm}^{-1}$ .
- Possible inhomogeneous distribution of TDs and SFs may explain surface morphology variations.

# HVPE LEO of m-GaN



- **Planar direct-growth films:**

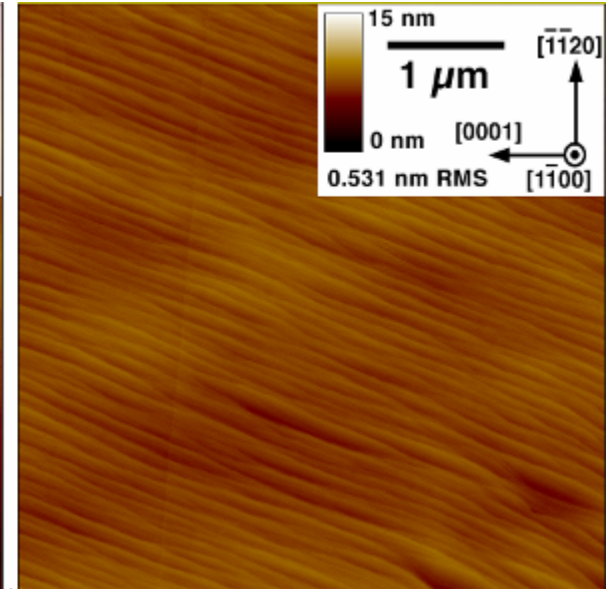
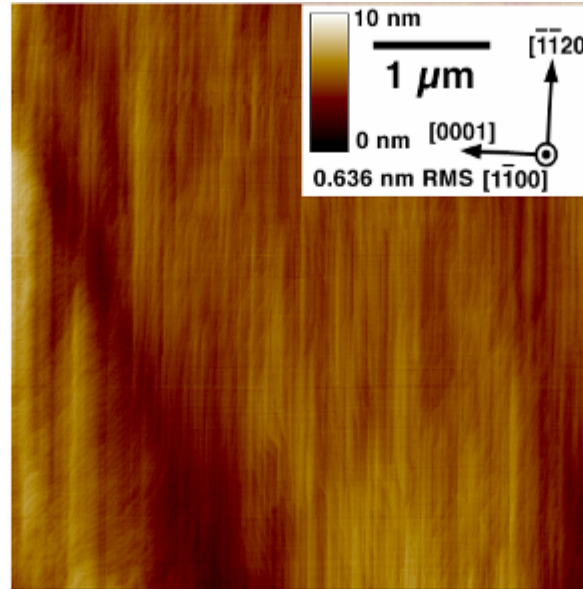
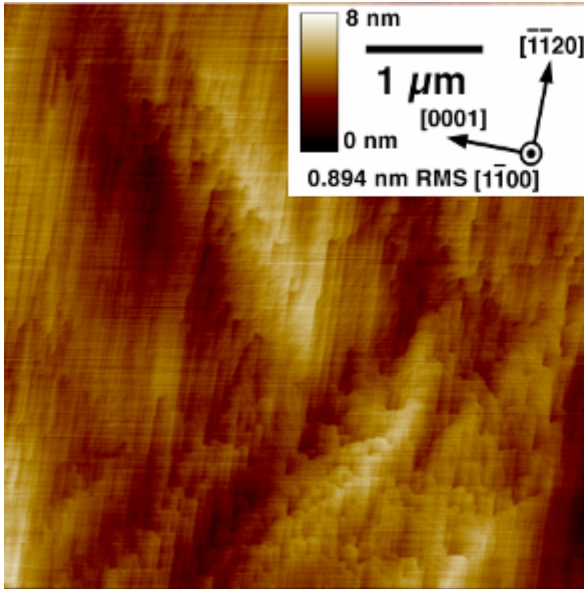
- Lattice mismatch, island coalescence  $\Rightarrow$  threading dislocations.
- Exposed (000 $\bar{1}$ ) planes in island/3D growth  $\Rightarrow$  basal plane stacking faults

- **Lateral epitaxial overgrowth:**

- Mask geometry affects growth direction.
- Natural growth habit: growth on *m*-planes preferred.
- <11 $\bar{2}$ 0>-oriented stripes (*a*-direction)  $\Rightarrow$  Growth on (0001) and (000 $\bar{1}$ ) planes (vertical sidewalls)

# HVPE LEO of m-GaN (cont.)

## AFM



- Direct growth:

- Slate morphology most prevalent.
- Ridge density  $\sim 10^5 \text{ cm}^{-1}$
- **Inhomogeneous distribution of ridges and pits.**

- LEO, <0001> Stripes:

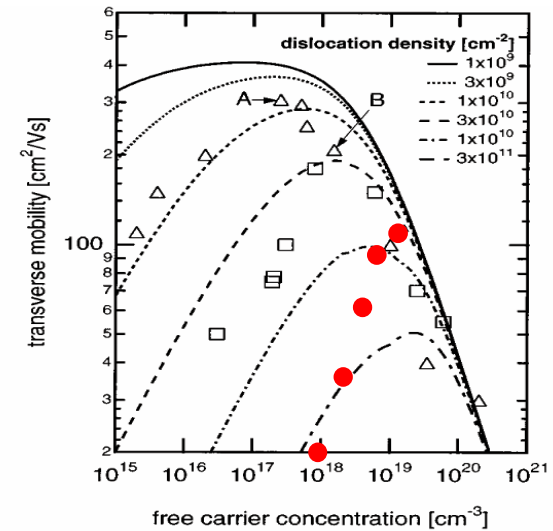
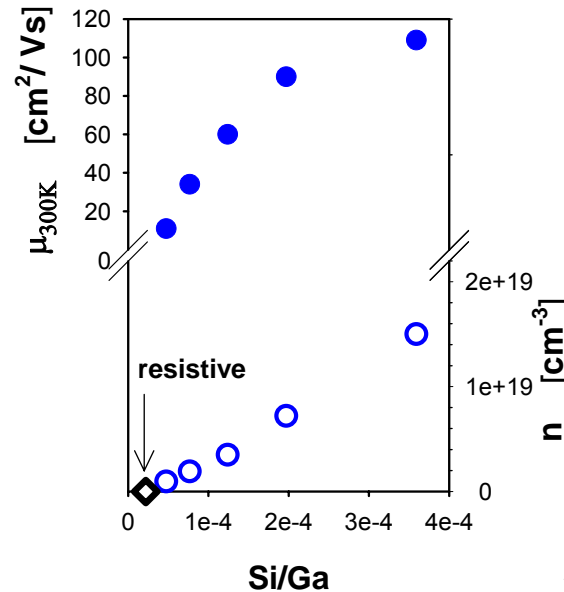
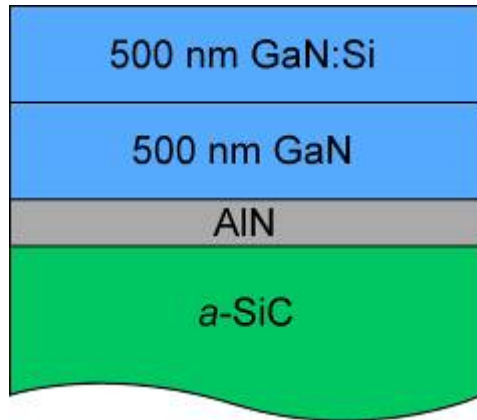
- Ridges remain, no pits.
- Roughness: 0.6 nm
- Wings TD-free.
- **SFs persist throughout wings.**

- LEO, <1120> Stripes:

- Ga-face wing TD and SF free.
- **Ridges eliminated, clear step edges on surface.**
- Roughness:  $\sim 0.5 \text{ nm}$

# n-Type Doping of a-GaN

- a-GaN on a-SiC:



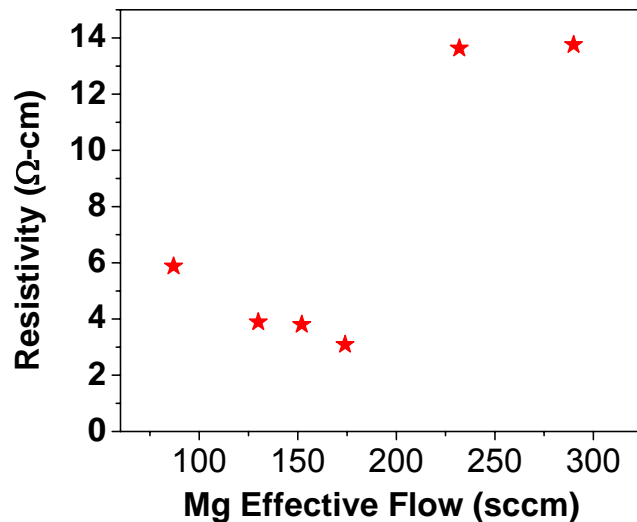
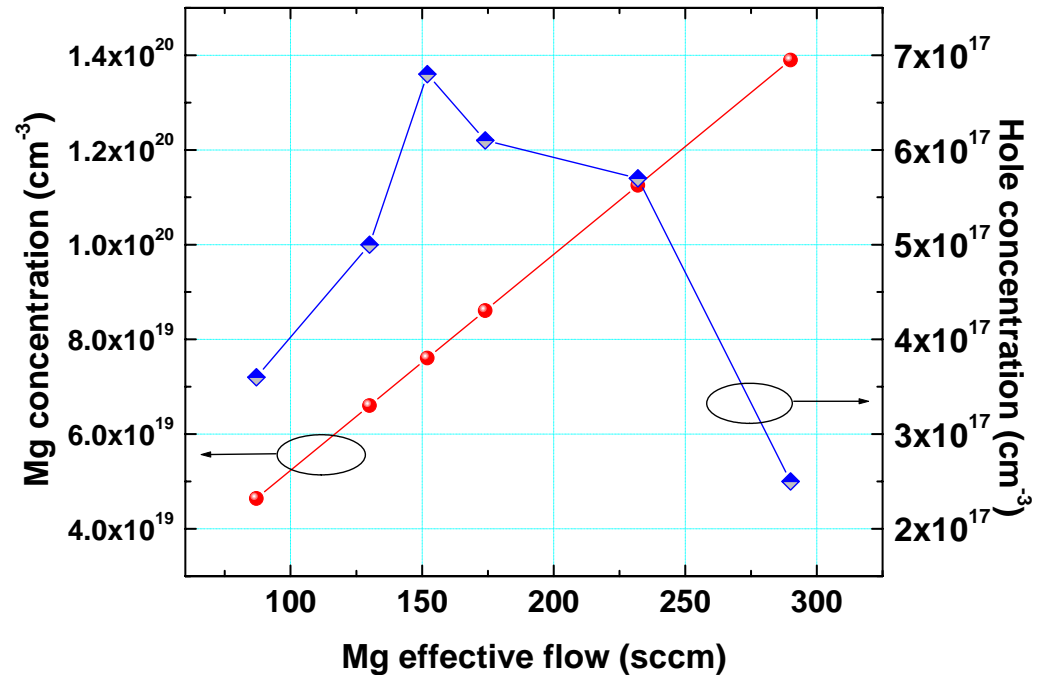
N.G. Weimann et al. *J. Appl. Phys.* 83 (1998) 3656

- Undoped GaN is resistive
- $n$  increases with Si/Ga ratio for  $n > 1 \times 10^{18} \text{ cm}^{-3}$
- Residual acceptor concentration on the order of  $1 \times 10^{18} \text{ cm}^{-3}$ 
  - Acceptors related to dislocations, stacking faults, and point defects
- $\mu$  increases with  $n$  (screening of defects)
  - at  $n = 1.5 \times 10^{19} \text{ cm}^{-3}$ ,  $\mu = 109 \text{ cm}^2/\text{V}\cdot\text{s}$

# p-Type Doping of *a*-GaN

- a*-GaN on *r*-sapphire:

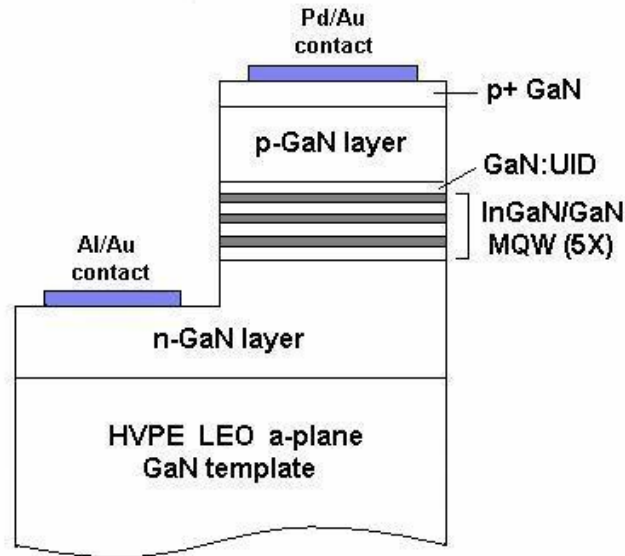
Mg Flow	$p$ ( $\text{cm}^{-3}$ )	$\mu$ ( $\text{cm}^2/\text{V}\cdot\text{s}$ )
87 sccm	$3.6\text{E}17$	3.0
130 sccm	$5.1\text{E}17$	3.2
152 sccm	$6.8\text{E}17$	2.5
174 sccm	$6.1\text{E}17$	3.3
232 sccm	$5.7\text{E}17$	1.0
290 sccm	$2.5\text{E}17$	1.8



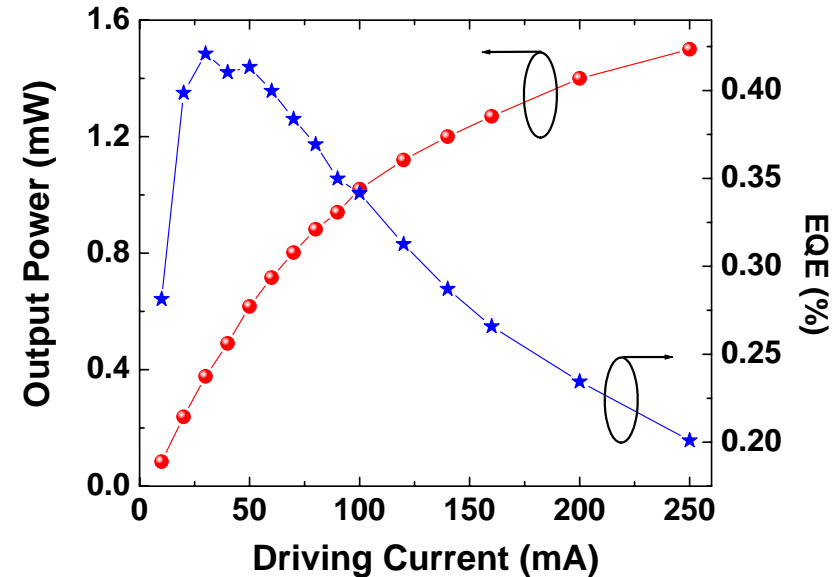
- [Mg] tracks  $\text{Cp}_2\text{Mg}$  effective flow**
- Reduction in hole concentration:**
  - Incorporation of Mg in electrically inactive form (e.g. precipitates)**
  - Formation of Mg-induced compensating defects**

# LED on HVPE LEO a-GaN

- Template: LEO HVPE a-GaN with  $2\mu\text{m}$  windows,  $8\mu\text{m}$  wings,  $\langle 1\bar{1}00 \rangle$  direction



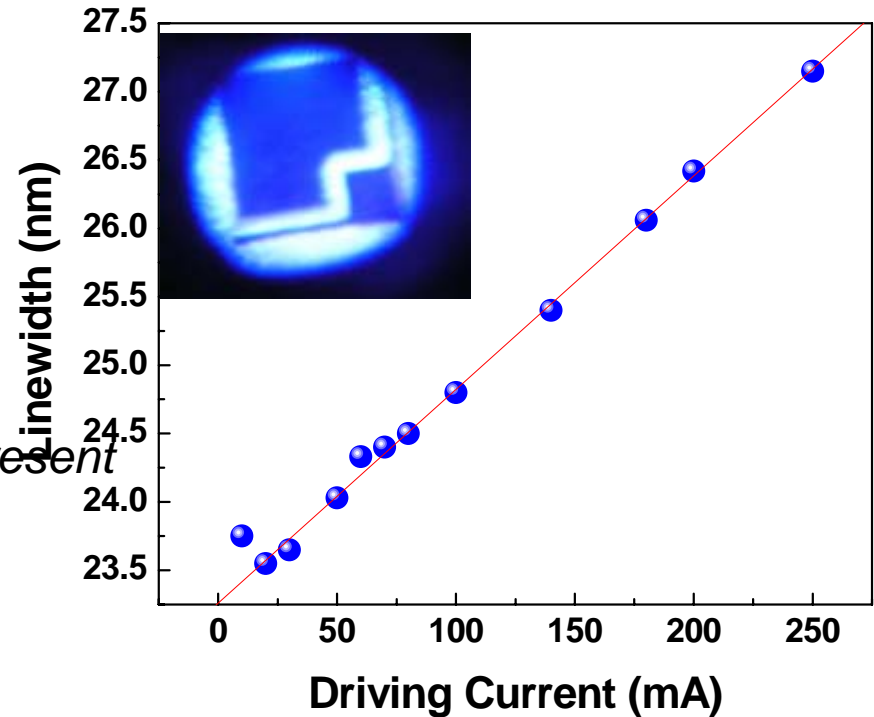
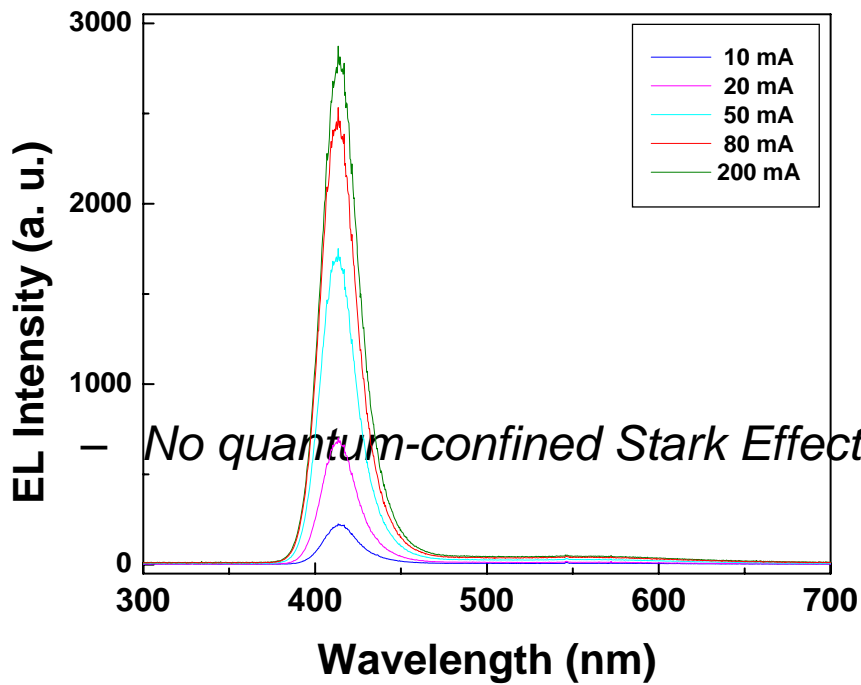
***n*-GaN:  $2.2\ \mu\text{m}$  ( $3 \times 10^{18}\ \text{cm}^{-3}$ )**  
***p*-GaN:  $0.3\ \mu\text{m}$  ( $6 \times 10^{17}\ \text{cm}^{-3}$ )**  
***n*-contact: Al/Au (30/200 nm)**  
***p*-contact: Pd/Au (3/200 nm)**



On-chip measurement:  
1.5 mW at 200 mA (unsaturated)

# *a*-GaN LED EL

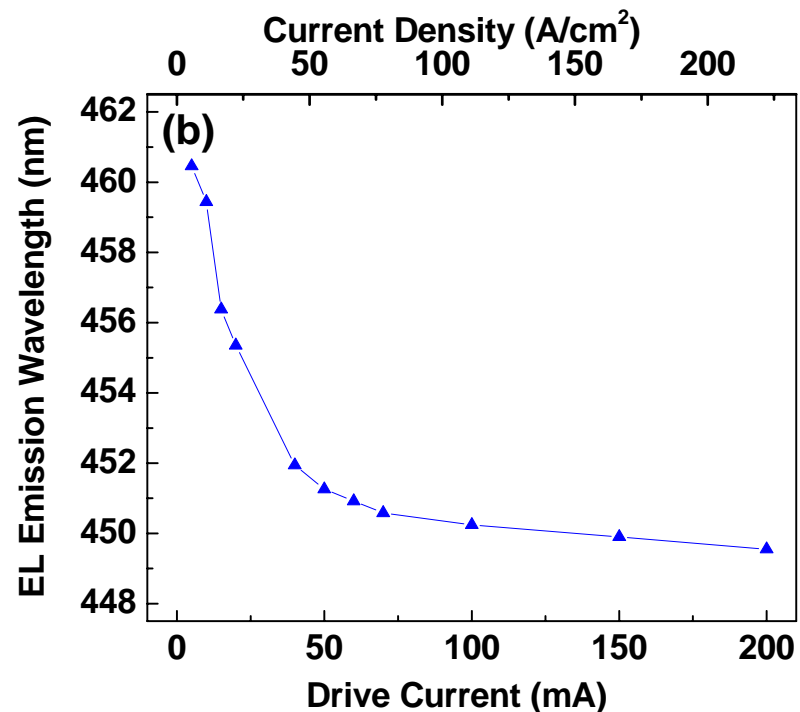
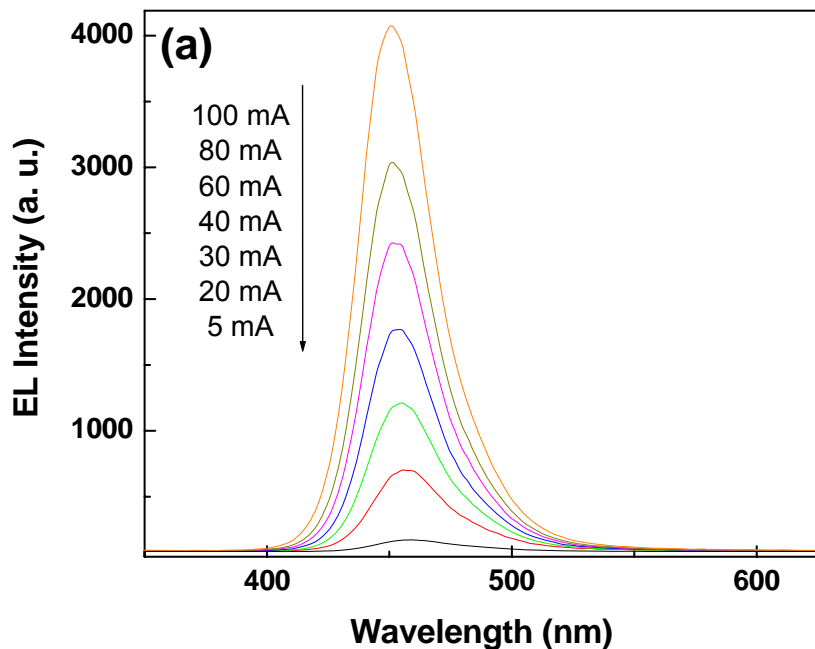
- Electroluminescence vs. current: no shift in peak position, little peak linewidth broadening



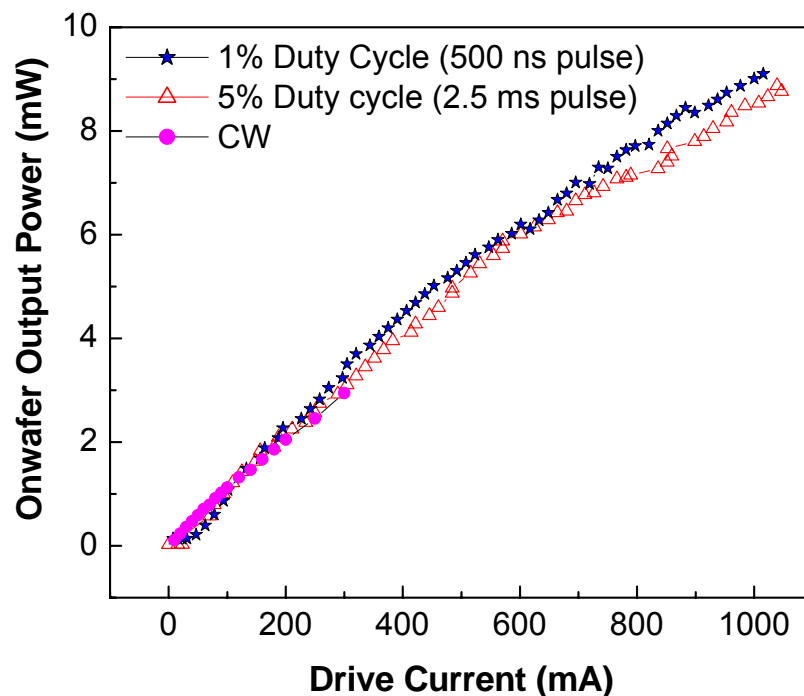
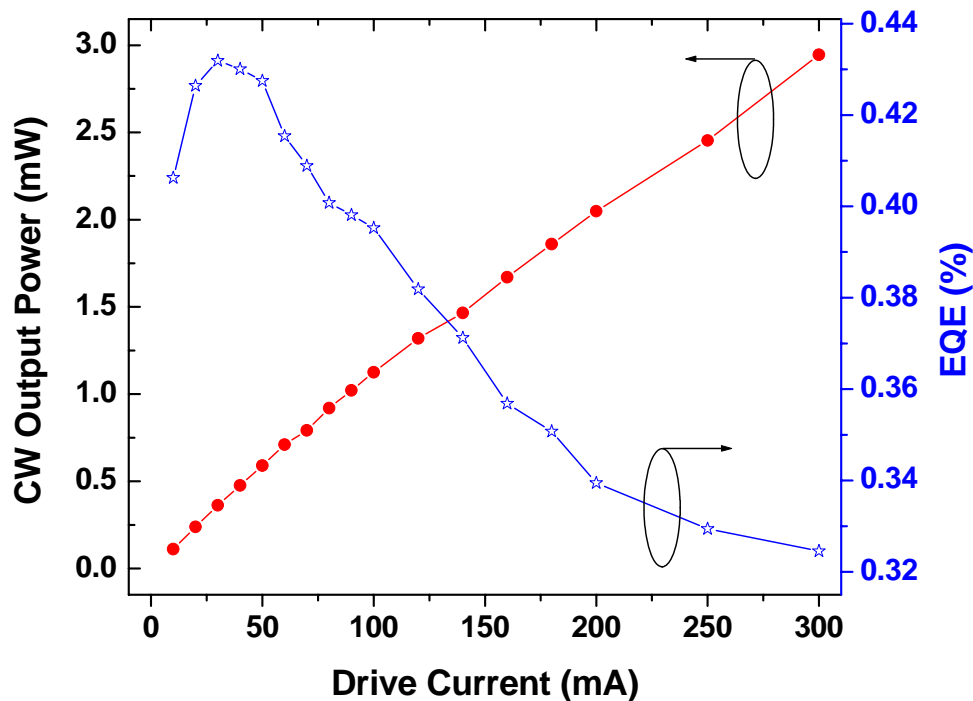
# LED on planar *m*-GaN (cont.)

- MOCVD 5-QW LED on 250  $\mu\text{m}$  free-standing planar HVPE *m*-GaN

- Turn-on voltage: 3-4 V
- Low on series resistance: 16  $\Omega$
- Ideality factor  $\sim 4$
- EL emission at 450 nm
- Peak shift observed at low current densities due to band filling



# Unpackaged m-GaN LED Results



- cw on-wafer output power at 300 mA : 2.95 mW (0.24 mW @ 20 mA)
- Max EQE of 0.43% at 30 mA drive current
- Saturation in output power **not** observed for higher cw drive currents
- Pulsed on-wafer output power at 1 A for 5% duty cycle: **8.5 mW**

# Packaged *m*-GaN LED Results

- **Unoptimized** chip packaged in standard T05 package
- Integrated optical power measured in integrating sphere
- Approx. **6 mW** at 200 mA
- Same slight emission peak shift vs. current, as for on-wafer testing

